Clim. Past Discuss., doi:10.5194/cp-2016-18, 2016
Manuscript under review for journal Clim. Past
Published: 15 February 2016

Climate of the Past Discussions

Detection and origin of different types of annual laminae in recent stalagmites from Zoolithencave, southern Germany: Evaluation of the potential for quantitative reconstruction of past precipitation variability

Dana Felicitas Christine Riechelmann[1], Jens Fohlmeister[2], Rik Tjallingii[3,4], Klaus Peter Jochum[5], Detlev Konrad Richter[6], Geert-Jan A. Brummer[4] and Denis Scholz[1]

[1]{Johannes Gutenberg-University Mainz, Institute for Geosciences, Johann-Joachim-Becher-Weg 21, D-55128 Mainz, Germany}

[2]{Ruprecht-Karls University Heidelberg, Institute for Environmental Physics, Im Neuenheimer Feld 229, D-69120 Heidelberg, Germany}

[3]{GFZ German Research Centre for Geosciences, Section Climate Dynamics and Landscape Evolution, Telegrafenberg Building C, D-14473 Potsdam, Germany}

[4]{NIOZ-Royal Netherlands Institute for Sea Research, Department of Marine Geology and Chemical Oceanography, Landsdiep 4, NL-1797 SZ 't Horntje (Texel), The Netherlands}

[5]{Max Planck Institute for Chemistry, Climate Geochemistry Department, Hahn-Meitner-Weg 1, D-55128 Mainz, Germany}

[6]{Ruhr-University Bochum, Institute for Geology, Mineralogy and Geophysics, Univeristätsstrasse 150, D-44801 Bochum, Germany}

Correspondence to: D. F. C. Riechelmann (riechelm@uni-mainz.de)

Abstract

An arrangement of three stalagmites from Zoolithencave (southern Germany) was analysed for different types of annual laminae using both microscopic and geochemical methods. The speleothems show visible laminae (consisting of a clear and a brownish, pigmented layer pair)

Clim. Past Discuss., doi:10.5194/cp-2016-18, 2016
Manuscript under review for journal Clim. Past
Published: 15 February 2016

as well as fluorescent and elemental laminae. The age of the speleothems was constrained to 1800 to 1970 AD by ^{14}C-dating of a charcoal piece below the speleothems, detection of the ^{14}C bomb peak, as well as counting of annual laminae. Dating by the ^{230}Th/U-method was impossible due to detrital contamination.

On the annual time-scale, the variability of Mg, Ba, and Sr is controlled by Prior Calcite Precipitation (PCP) resulting in lower values during the wet season (autumn/winter) and vice versa. Yttrium and P are proxies for soil activity and are enriched in the brownish, pigmented layers. However, Y and P are also influenced by detrital content superimposing the soil activity signal. Aluminium and Mn are proxies for detrital content.

Lamina thickness shows a significant correlation with the amount of precipitation of previous December and current January, February, March, April, May, and December (DJFMAMD) recorded at the nearby meteorological station Bamberg. Thus lamina thickness is a proxy for past precipitation, which is confirmed by the good agreement with a precipitation reconstruction based on tree-ring width from the Bavarian forest. This highlights the potential of these speleothems for climate reconstruction at annual resolution.

1 Introduction

In the last decade, archives containing high-resolution climate proxies, which reflect past climate variability on a time-scale relevant for civilisation, have achieved increasing attention (e.g., Büntgen et al., 2011; Kennett et al., 2012). High-resolution climate reconstructions for central Europe are mostly available from tree-rings span the last 2000 years (e.g., Wilson et al., 2005; Büntgen et al., 2008; Trouet et al., 2009; Esper et al., 2012). Tree-ring records covering longer time spans such as the entire Holocene are rare (Spurk et al., 2002; Friedrich et al., 2004) and hold the problem of preserving low frequency climate signals. Speleothems, such as stalagmites and flowstones, can grow continuously for several thousand years. They can be precisely dated by the ^{230}Th/U-method (e.g., Richards and Dorale, 2003; Scholz and Hoffmann, 2008) and provide up to annual-resolution climate proxies. Therefore, they have large potential to extend the existing tree-ring records (Tan et al., 2006). Some speleothems show annual laminae and have the potential for annually or even seasonally resolved climate reconstruction (Brook et al., 1999; Proctor et al., 2002; Boch and Spötl, 2008; Mattey et al., 2008; Hardt et al., 2010; Orland et al., 2012; Myers et al., 2015; Ridley et al., 2015).

Typically, five types of annual laminae can be observed in speleothems: i) visible laminae with a white and a dark/clear layer representing one year (Genty and Quinif, 1996; Scholz et al., 2012; Van Rampelbergh et al., 2014), ii) fluorescent laminae induced by humic and fulvic acid (van Beynen et al., 2001; Proctor et al., 2002; Shopov, 2003; Sundqvist et al., 2005), iii) elemental laminae visible in cyclic (seasonal) changes in the concentration of specific elements (Roberts et al., 1998; Huang et al., 2001; Treble et al., 2003; Johnson et al., 2006; Borsato et al., 2007; Smith et al., 2009), iv) stable carbon and oxygen isotope laminae visible in changes in the $\delta^{13}C$ and $\delta^{18}O$ values over an annual cycle (Mattey et al., 2008; Baker et al., 2011; Boch et al., 2011; Van Rampelbergh et al., 2014; Myers et al., 2015; Ridley et al., 2015), and v) mineralogical laminae consisting of calcite-aragonite pairs representing one year (Railsback et al., 1994; Baker et al., 2008). All types of laminae have been analyse in several studies and their potential for reconstruction of climate variability evaluated. Visible annual laminae in speleothems can be induced by cave ventilation, which controls the super saturation of the drip water with respect to calcite via modulation of the pCO_2 of in the cave air. Cave ventilation is controlled by the temperature difference between outside atmospheric and cave air and may result in a temperature signal in $\delta^{13}C$ and $\delta^{18}O$ speleothem records (Boch et al., 2011). In addition, the annual cycle in the concentration of Mg, Sr, Ba, and/or P were used both as temperature (Mattey et al., 2008) or precipitation proxies (Roberts et al., 1998; Huang et al., 2001; Treble et al., 2003). The lamina thickness of both visible and fluorescent laminae were used as proxies for past precipitation and water excess (Genty and Quinif, 1996; Baker et al., 1999; Brook et al., 1999; Proctor et al., 2000; Boch and Spötl, 2008) or temperature (Frisia et al., 2003; Scholz et al., 2012).

In this study, we analysed an arrangement of three small stalagmites from Zoolithencave, southern Germany, for their visible, fluorescent, and elemental laminae. The aims of this study are i) to test the potential of different analytical methods to detect annual laminae in speleothems, ii) analyse the origin of the different types of laminae, and iii) evaluate their potential as climate proxies.

2 Cave setting

Zoolithencave (49°47’ N, 11°17’ E) is located in the Franconian Alb, south-eastern Germany, and developed in the Upper Jurassic Franconian Dolomite (Fig. 1). The dolomitisation of this massive spongal reef limestone already started in the Upper Jurassic (Meyer, 1972). The first

Clim. Past Discuss., doi:10.5194/cp-2016-18, 2016
Manuscript under review for journal Clim. Past
Published: 15 February 2016

karstification of the dolomite occurred predominantly along fissures with NW-SE and NE-SW orientation during the uplift of the Franconian Alb at the transition from the Jurassic to the Cretaceous. The main phase of karstification took place in the Quaternary and coincided with the further uplift of the Franconian Alb and erosion by rivers (Groiß, 1988).

The Zoolithencave is famous for its paleontological inventory, which was first described by Esper (1774) and Rosenmüller (1794). Bones of several Pleistocene mammals were found, and the cave is the first location where cave bear (*Ursus spelaeus*) bones were found. Further archaeological excavations found charcoal and pottery from the Iron Age, and an ash layer in a flowstone was dated to the late Mesolithicum (Rosendahl, 2005). This proves human utilisation of the cave. Zoolithencave was intensively studied during the late 18th to early 20th century due to its paleontological inventory. The second phase of scientific investigation started in 1971 when further parts of the cave where discovered and paleontological analyses were performed by, for instance Groiß (1979) and Diedrich (2014). At the same time, speleological studies were conducted (e.g., Tietz, 1988; Wurth et al., 2000; Wurth, 2002; Richter et al., 2014; Riechelmann et al., 2014).

The cave entrance is located 455 m above sea level on the north-east facing slope of the Hohle Berg. The peak of the Hohle Berg is 469.9 m above sea level and forms a small karst plateau. The average rock overburden of the cave is 15-20 m, which is covered by soil consisting of a 15 cm thick humic A-horizon and a > 30 cm thick loamy B-horizon (Wurth, 2002). The vegetation above the cave mainly consists of deciduous forest (i.e., predominately beech).

3 Material and Methods

3.1 Stalagmite Zoo-rez

Stalagmite Zoo-rez is an arrangement of two stalagmites with a distance of 7 cm between their tops, which grew in entrance hall of Zoolithencave. Zoo-rez-1 has a height of 3 cm, whereas Zoo-rez-2 is 2.7 cm high. A third, 2.5 cm-high stalagmite (Zoo-rez-3) grew at close distance. All three stalagmites were sampled in August 1999 (Fig. 2; Wurth (2002)). The base of the arrangement of Zoo-rez-1 and -2 consists of cave loam, as well as sinter and charcoal pieces, which are consolidated by calcite. The stalagmite was fed by an active drip when it was sampled suggesting recent growth.

3.2 Dating methods

Two samples (ca. 300 mg) from the top and the base of Zoo-rez-1 (Fig. 3a), respectively, were drilled for ^{230}Th/U-dating using a hand held dental drill. The samples were dissolved in 7N HNO_3 and spiked with a mixed ^{229}Th-^{233}U-^{236}U spike solution. The Th and U fractions were separated by ion-exchange column chemistry (see Yang et al. (2015), for details) and subsequently analysed using a Nu Plasma MC-ICP mass-spectrometer (*Nu Instruments Ltd., Wrexham*) at the Max Planck Institute for Chemistry, Mainz. For further methodological and analytical details, the reader is referred to Obert et al. (accepted).

All activity ratios and ^{230}Th/U-ages were calculated using the half-lives of Cheng et al. (2000). To account for potential detrital contamination, corrected ages were calculated assuming an upper continental crust ^{232}Th/^{238}U weight ratio of 3.8 ± 1.9 (Wedepohl, 1995) and secular equilibrium between ^{230}Th, ^{234}U, and ^{238}U.

A piece of charcoal found at the base of Zoo-rez-2 (Fig. 3b) was analysed by accelerator mass spectrometer (AMS) ^{14}C-dating at the Curt-Engelhorn-Zentrum for Archeometry gGmbH, Mannheim, Germany. The sample was prepared with the ABA-method (HCl/NaOH/HCl), whereat the insoluble components were burned and the resulting CO_2 catalytically reduced to graphite. The ^{14}C content was determined with a MICADAS accelerator mass spectrometer (Synal et al., 2007). In addition, three calcite samples from the top of stalagmite Zoo-rez-1 (Fig. 3a) were analysed for their ^{14}C content in order to detect the atmospheric ^{14}C bomb peak. These samples were dissolved in vacuo and subsequently reduced to graphite at 575°C under a H_2 atmosphere. The measurements were performed using the same setup as for the charcoal sample.

3.3 Fluorescence and polarisation microscopy and determination of lamina thickness

Fluorescence microscopy was performed on thin sections of 30 µm thick using a *Leica DM4500P* microscope, which is equipped with a *Canon Eos 60D* camera at the Institute for Geology, Mineralogy and Geophysics at Ruhr-University Bochum. For UV-luminescence, a BP360/40 excitation filter, a dichromatic mirror of 400 nm and an LP425 suppression filter were used. Polarisation microscopy was performed with a *Leica DM750P* microscope. The thin sections were further scanned with a *Colorview I* camera (*Olympus)* installed on an

Clim. Past Discuss., doi:10.5194/cp-2016-18, 2016
Manuscript under review for journal Clim. Past
Published: 15 February 2016

Olympus EX51 microscope, which is equipped with a *Märzhäuser LPT15* microscope stage and a *Plan N20x* objective resulting in high resolution pictures. Determination of lamina thickness on these pictures was performed using the software analySIS pro (*Olympus Soft Imaging Solutions*). On Zoo-rez-1, three tracks were measured. On Zoo-rez-2 and -3 one track each was measured. The microscopy tracks followed the LA-ICPMS tracks (Fig. 3, see also section 3.5). Cross dating of the lamina thickness of the different tracks was performed using the tree-ring analysis software tools TSAP-Win® (*RINNTECH, Heidelberg*) and COFECHA (Holmes, 1983).

3.4 LA-ICPMS measurements for elemental concentrations

The elemental concentration of the three stalagmites was determined with an Element2 ICP mass spectrometer (*ThermoScientific, Waltham, USA*) equipped with a high energy Nd:YAG laser ablation system (λ = 213 nm) (*New Wave, Fremont, USA*). The reference material used for calibration was NIST SRM 612, a synthetic glass with a high trace element content (Jochum et al., 2011). The spot size of the laser beam was 110 µm, the puls repetition rate 10 Hz and the scan speed 10 µm/s. The elemental concentrations were normalised using Ca as an internal standard. In total, 33 elements were measured: Na, Mg, Al, Si, P, Ca, Ti, Mn, Fe, Cu, Zn, Rb, Sr, Y, Cd, Ba, La, Ce, Pr, Nd, Sm, Eu, Gd, Tb, Dy, Ho, Er, Tm, Yb, Lu, Pb, Th and U. Seven (Mg, Al, P, Mn, Sr, Y, Ba) revealed reliable concentrations well above the detection limit. As for the microscopy tracks, three tracks on stalagmite Zoo-rez-1, and one track each on Zoo-rez-2 and -3 were measured (Fig. 3).

3.5 UV-Luminescence Scanning

UV-luminescence of the three speleothems was measured with an *Aavatech* core scanner at the NIOZ (Texel, Netherlands). Images were acquired with a resolution of 70 µm/pixel using a JAI CCD camera, equipped with a beam splitter separating the red, green and blue colour channels (Grove et al., 2010). The speleothem samples were irradiated with a 365 nm UV-LED lamp to initiate the luminescence. The CCD camera was equipped with a 435 nm cut off filter to avoid recording of reflecting light of the initial light source. RGB colour information was obtained from the images along selected transects, corresponding to the elemental and lamina thickness transects, using the software Line Scan 2.0 of the Avaatech scanner.

3.6 Data analysis

Principal Component Analysis (PCA) and wavelet analysis of the elemental data series were performed using the software *PAST (Hammer et al., 2001)*. For both analyses, the data were normalised. In addition, Pearson correlation coefficients (r) were calculated between the different elemental data series as well as between the proxy series and different climate parameters. Wiggle matching of the different tracks (Mg content, UV-luminescence, and lamina thickness) was conducted using the software *AnalySeries (Paillard et al., 1996)*. Interpolation of the elemental and UV-luminescence data series as well as the calculation of mean curves were performed with R (R Core (Team, 2015). Detrending of the lamina thickness and mean annual Mg records with a 10 point FFT (Fast Fourier Transformation) filter was performed using Origin®.

4 Results

4.1 Visible laminae

Visible laminae in Zoo-rez appears as layer pairs consisting of a clear layer and a layer with brownish pigmentation (Fig. 4a). Counting these laminae along the three tracks of Zoo-rez-1, results in 124, 161, and 135 laminae, respectively. In Zoo-rez-2, we counted 165 laminae, and in Zoo-rez-3, 144 laminae. The mean laminae thickness varies from 129 (Zoo-rez-2) to 203 µm (Zoo-rez-1, track 1). The minimum lamina thickness varies from 25 (Zoo-rez-1, track 2) to 56 µm (Zoo-rez-1, tracks 1 and 3), whereas the maximum lamina thickness ranges from 388 (Zoo-rez-2) to 917 µm (Zoo-rez-3). Further microscopic analysis of the thin sections of the three stalagmites did not provide any evidence for growth stops. Therefore, continuous growth is assumed. The crystal fabric of all stalagmites is columnar facicular optic and only some patches of Zoo-rez-1 show a columnar radiaxial fabric (Richter et al., 2011; Frisia, 2015).

4.2 Chronology of stalagmite Zoo-rez

The corrected ^{230}Th/U-ages determined for Zoo-rez-1 are of 4670 ± 1000 years BP (this refers to 2014 AD) for the sample taken at 0.3 cm distance from top (dft) and 340 +3314/-295 years

BP for the sample from 1.4 cm dft (Table 1). The very large age uncertainties result from the large degree of detrital correction, which results in differences between corrected and uncorrected ages of up to 5000 years (Table 1). This is a result of the low U and elevated ^{232}Th content of the two samples and is also evident from a very low (^{230}Th/^{232}Th) activity ratio, which range from 0.9 to 2.6 (Table 1). For (^{230}Th/^{232}Th) ratios lower than 20, a correction for detrital contamination is necessary (Schwarcz, 1989). However, in particular for very young samples, such as stalagmite Zoo-rez-1, the conventionally applied bulk Earth correction is not adequate and more elaborate methods are required (Ku and Liang, 1984; Schwarcz and Latham, 1989; Bischoff and Fitzpatrick, 1991; Przybylowicz et al., 1991; Kaufman, 1993; Ludwig, 2003; Pons-Branchu et al., 2014; Wenz et al., in review). Thus, the two ^{230}Th/U-ages determined for stalagmite Zoo-rez-1 cannot be considered reliable, which is also obvious from the age inversion (i.e., the age close to the surface is older than the age at the base of the stalagmite, Table 1). As a consequence, other methods to establish the chronology of stalagmite Zoo-rez have to be used.

The ^{14}C-age of the charcoal piece from the base of stalagmite Zoo-rez-2 is 165±21 years BP (refers to 1950 AD), with a calibrated 1σ-range of 1671-1951 AD (Table 2). Calibration was performed with INTCAL13 (Reimer et al., 2013) and SwissCal 1.0 (L. Wacker, ETH-Zürich). Furthermore, the ^{14}C-activity of three samples from the top of stalagmite Zoo-rez-1 was determined in order to detect the atmospheric bomb peak (Hua et al., 2013). This atmospheric bomb peak was induced by the above ground atomic bomb tests in 1945-1963 AD. The ^{14}C from this tests was circulated worldwide by the atmosphere and reached for example stalagmites via rain and drip water. The ^{14}C activity detected in a speleothem is always lower than in the atmosphere, due to dissolution of the hostrock which contains carbon as well. The sample from 0.8 mm dft shows the highest ^{14}C-activity (Fig. 5). The subsequent decrease in atmospheric ^{14}C-activity has not been observed in the stalagmite suggesting that Zoo-rez did not grow until 1999 AD (the year of sampling). The maximum of speleothem bomb spikes appears to be near the atmospheric peak as long as the increase in radiocarbon is large. For speleothems with a smaller increase in ^{14}C the maximum in the speleothem is delayed. This is explained by the age spectrum of SOM (Fohlmeister et al., 2011). Since the increase in ^{14}C in Zoo-rez is large (compare e.g., Noronha et al., 2015), the peak is near the maximum of the atmospheric ^{14}C values. Thus, we suggest that the highest ^{14}C value corresponds to about 1967 AD and attributed a 5 years uncertainty. It follows that the stalagmite stopped growing around 1970 AD ± 5 years by adjusting the ^{14}C sampling site by lamina counting. The age of the charcoal, which must be older than the stalagmite growing on top, is in good agreement with the number of 124 to 165 layers counted. Therefore, stalagmite Zoo-rez most likely grew during the last 150-200 years and shows visible annual laminae.

4.3 Elemental laminae

Seven elements (Mg, Al, P, Mn, Sr, Y, Ba) revealed reliable concentrations well above the detection limit. The element records obtained from the five sampling tracks were compared by calculation of correlations that reveal in two groups of elements. The first group reveals positive correlation with each other contains of the elements Mg, Sr, and Ba, whereas the second group shows positive correlations with each other contains of Al, P, Mn, and Y (Table 3). This is confirmed by the results of the Principle Component Analysis (PCA; von Storch and Zwiers, 2002; Navarra and Simoncini, 2010), performed with the normalised elemental concentrations, with Mg, Sr, and Ba grouping together, as well as Al, P, Mn, and Y. Only for the PCA of Zoo-rez-2 Al and Mn as well as P and Y form two different groups (Fig. 6).

The time series of Mg, P, Sr, Y, and Ba show a cyclicity with higher and lower values (Figs. 7a and b). Aluminium and Mn do not show this pattern (Fig. 7c). However, both elements show extreme concentrations (i.e., spikes) in some sections of the speleothems and very low concentrations in other parts (Fig. 7c). The observed cyclicity, which probably results from annual variations in elemental supply, is most pronounced for Mg (Fig. 7a). Phosphorus, Sr, Y, and Ba show several spikes superimposed on the cyclicity, which is not the case for Mg (Figs. 7a and b). Therefore, potential annual elemental lamination seems to be most pronounced for Mg. In order to test whether the observed cyclicity is annual, wavelet analysis has been performed for the five Mg time series (cf., Smith et al., 2009). The five wavelet plots show a continuous cyclicity in the range of 64 to 256 µm over the whole length of all measuring tracks (Fig. 8), which is in agreement with thickness of the visible laminae (compare section 4.1). This strongly suggests that the observed cyclicity of Mg concentration reflects an annual signal. Due to the observed positive correlation and grouping in the PCA between Mg, Ba, and Sr (Table 3), it is likely that the variability of all three elements reflect an annual signal.

4.4 Luminescent laminae

Clim. Past Discuss., doi:10.5194/cp-2016-18, 2016
Manuscript under review for journal Clim. Past
Published: 15 February 2016

The pixel resolution of UV-luminescence scanning does not allow an annual signal (cf., Fig. 14) as the mean lamina thickness of the visible layers observed for the five different tracks of Zoo-rez is in the range of two pixels (compare section 4.1). However, this method is not really suitable to detect annual laminae in speleothem Zoo-rez, but rather for multi-annual scale fluctuations.

UV-luminescence microscopy clearly shows a lamination, with the brownish layers exhibiting a stronger luminescence than the clear layers under UV light (Fig. 4). Pronounced brownish layers provide a stronger and more easily detectable luminescence than less pronounced layers, which confirms the observations of the visible laminae. Therefore, fluorescence microscopy does not provide additional information for stalagmite Zoo-rez.

5 Interpretation and Discussion

5.1 Chronology

Based on the five laminae thickness tracks, a chronology with an annual resolution was built by visual cross-dating using the tree-ring software TSAP-Win®. Due to the geometry of stalagmite Zoo-rez-1, the laminae get thinner and even disappear with increasing distance from the growth axis (Fig. 3a). This is especially the case for those sections of Zoo-rez-1 showing no clear plateau (Fig. 3a) and is probably also the major reason for the different number of laminae counted for the three different tracks on Zoo-rez-1. Track 2 is closest to the growth axis and should therefore have less missing laminae than the other tracks. This is confirmed by the observed number of laminae (161 for track 2 and 124 and 135 for track 1 and 3, respectively). Consequently, tracks 1 and 3 were cross-dated to track 2, and the corresponding number of missing laminae was inserted into the chronology using TSAP-Win. We assumed a lamina thickness of 10 µm for the missing laminae, which is the accuracy of the thickness determination. In total, 19 missing laminae were inserted into track 1, nine laminae into track 2 and 11 into track 3. Also in the master track 2 nine laminae were inserted, which most likely is due to irregularities in the continuous growth of the laminae over the stalagmite surface. Furthermore, the total amount of laminae after the cross-dating differ for the different tracks, which is due to more or less clear laminae structure near to the base part of the stalagmites. We note that this procedure is a standard technique in tree-ring research (Fritts, 1976; Schweingruber, 1983; Speer, 2010). Subsequently, the two individual tracks on

Zoo-rez-2 and -3 were cross-dated to the mean curve of the three tracks on Zoo-rez-1. Into track Zoo-rez-2, six laminae were inserted, and into track Zoo-rez-3, eleven laminae were inserted. As in tree-ring cross-dating, each inserted laminae is present in at least one of the tracks and, thus not missing in all tracks. Subsequently to visual cross-dating of the five tracks, the chronology was checked using the tree-ring software COFECHA (Holmes, 1983). This check calculates the series intercorrelation, which is the mean of the correlations of each series with the mean of the remaining series. For our chronology, the series intercorrelation is 0.51. Furthermore, COFECHA calculates the correlation of the series with the mean of the other series to detect potential dating errors by shifting by maximum 10 years in both direction using segments of 50 years with an overlap of 25 years. For some segments, the correlation was lower than for the shifted segment. However, these correlation coefficients were not significantly higher and do therefore, not suggest an error during cross-dating (Holmes, 1983; Speer, 2010). In summary, the cross-dating procedure results in a chronology of 171 years, which represents the mean annual lamina thickness of the five series. Note that neither additional missing laminae nor laminae not representing a full year can be excluded. However, due to the five series and the cross-dating, which do not show distinct dating errors, this chronology can be considered as relatively robust.

To assign an absolute age to the floating chronology, the ^{14}C-ages were used (see section 4.2) and assuming annual laminae in the stalagmite, the age of the uppermost layer was set to 1970 AD. This assumes a fast percolation of the rain water into the cave, which is supported by the low (10-12 m) rock overburden of the entrance hall of Zoolithencave. A short residence time in the aquifer is a general prerequisite for the formation of annual laminae in speleothems (Baker et al., 2008). Another factor, potentially producing annual laminae in speleothems is strong cave ventilation resulting in a strong annual variability of cave pCO_2 (Huang et al., 2001; Mattey et al., 2008; Boch et al., 2011). However, this can be excluded for Zoolithencave because monitoring results show that cave pCO_2 is relatively low (530-1662 ppmV) in the entrance hall and does not vary by more than 1000 ppmV throughout the year (Meyer, 2014). Hence, the observed annual lamination in stalagmite Zoo-rez is most likely related to annual changes in drip water composition (Roberts et al., 1998; Huang et al., 2001; Treble et al., 2003; Wassenburg et al., 2012).

The age of the lowermost lamina of stalagmite Zoo-rez is 1800 AD, which is in a good agreement with the calibrated 1σ-range of the ^{14}C dating of the charcoal resulting in 1671-1951 AD, whereas one possible calibration range spikes around 1800 AD. Due to the good agreement of the number of counted laminae with the ^{14}C-dating results, the number of missing and/or double-counted years should be very low and can be neglected. Nevertheless, the absolute age of the chronology may vary by a few years (cf., Shen et al., 2013). The resulting annually resolved chronology for Zoo-rez (Fig. 9) can be further used to assign a chronology to the proxy signals.

5.2 Wiggle matching and data interpolation

Due to the potential annual nature of Mg cycles, wiggle matching between the individual Mg series was performed using the software *AnalySeries.* As for the visible laminae (compare section 5.1), track Zoo-rez-1.2 was chosen as the master series, which shows the largest number of visible layers and is closest to the growth axis (Fig. 3a). All other Mg tracks were wiggle matched on this master track (Fig. 10), which leads to an increase in the correlation coefficients between the individual tracks to of r = 0.43 to r = 0.49. This is substantially higher than correlation coefficients prior to wiggle matching, which range from r = 0.10 to r = 0.24. On average, the data points on track Zoo-rez-1.1 were shifted by 179 µm, by 502 µm on track Zoo-rez-1.3, by 344 µm on Zoo-rez-2, and by 1253 µm on Zoo-rez-3. The relatively large shift on Zoo-rez-3 is probably related to the largest distance of this track from the master track (Zoo-rez-1.2). Subsequently to wiggle matching, a mean curve of all five Mg signals was calculated. This mean Mg series was cut off at the end of the shortest series (i.e., Zoo-rez-2). Lamina thickness was determined on thin sections, which were produced from the opposite sides of the slices used for the elemental measurements. Therefore, it is not possible to use the individual lamina thickness chronologies to construct an age model for the Mg individual signals. Thus, the lamina thickness chronology was wiggle matched to the mean Mg curve. The laminae consist of a clear layer and brownish-pigmented layer. The clear layer corresponds to higher Mg concentration and the brownish pigmented to lower Mg concentration. The end of the brownish pigmented layer represents approximately the end of the flush in of humic particles. Therefore, this boundary for the laminae in the mean Mg record was set in the middle of the increasing slope of the cycle in the Mg concentration (Fig. 11). The average shifting of the laminae boundaries was 44 µm (Fig. 11). Since both the lamina thickness and the Mg curve are based on five individual tracks, we consider the chronology of the resulting proxy time series as relatively robust. Since the resolution of the Mg curve is much higher than that of the lamina thickness series, the mean Mg concentration

Clim. Past Discuss., doi:10.5194/cp-2016-18, 2016
Manuscript under review for journal Clim. Past
Published: 15 February 2016

Climate of the Past
Discussions

of the individual years was calculated. This results in an annually resolved Mg time series (Fig. 12).

The G/B ratio series of the UV-luminescence scanning analyses from the three tracks on Zoo-rez-1 were wiggle matched in the same way as the Mg curves and a mean curve was calculated. Due to the lower resolution of 70 µm/pixel of the G/B ratios, Mn, and Y concentration series need to be interpolated on the scale of the G/B ratios to compare these series.

5.3 Interpretation of the proxy signals in terms of past climate variability

5.3.1 Elemental laminae

Magnesium, Ba, and Sr concentration are significantly correlated with each other (Table 3) and also form a group in PCA (Fig. 6). The Mg, Ba, and Sr content of Zoo-rez is higher in spring and summer (drier conditions, clear laminae) and lower in autumn and winter (wetter conditions, brownish laminae). This is probably induced by prior calcite precipitation (Treble et al., 2003; Smith et al., 2009) occurring in air filled pockets and cavities in the aquifer above the cave. PCP increases the Mg, Sr, and Ba content of the drip water and, hence, in speleothem calcite (Fairchild et al., 2006). The occurrence of air filled cavities and pockets in the karst aquifer is most pronounced in the summer season, which results in increased PCP (Wassenburg et al., 2012). Therefore, Mg, Ba, and Sr concentration is a proxy for recharge of the karst aquifer and directly linked to precipitation. These three elements, thus, reflect the annual cycle of infiltration with higher amounts of infiltration during autumn and winter and lower infiltration in spring and summer. During spring and summer, evapotranspiration reduces the amount of infiltrating rain water (Wackerbarth et al., 2010; Mischel et al., 2015). Magnesium and Sr concentration were also determined for a small section of another stalagmite from Zoolithencave by Wurth (2002). The results show a higher Mg and Sr content of the clear layers and a lower content of the brownish layers. The brownish layers probably result from a flush of organic material into the cave during autumn (Huang et al., 2001; Sundqvist et al., 2005) when the recharge of the aquifer increases after the summer, which is characterised by strong evapotranspiration (Mischel et al., 2015).

The second group identified by the PCA consists of Al, Mn, P, and Y. An exception is Zoo-rez-2, where Al and Mn as well as P and Y form two different groups (Fig. 6d). Phosphorus and Y are interpreted as proxies for vegetation density and soil activity (Treble et al., 2003;

Borsato et al., 2007; Wassenburg et al., 2012). Therefore, their concentration should be elevated in the brownish layers reflecting increasing recharge. Yttrium and P are positively correlated in all tracks (Table 3), supporting this interpretation. For track Zoo-rez-2, a negative correlation between Mg and Y is observed (Table 3 and Fig. 13) (cf., Mattey et al., 2008). For the others tracks, this relationship is only observed for some sections. This is probably a result of detrital contamination, which is also visible in the positive correlations of P and Y with Al and Mn (Wassenburg et al., 2012) as well as in the grouping of these elements in the PCA (Fig. 6), because Al and Mn are proxies for detrital material. In Zoo-rez-2, only a low correlation of P and Y with Al and Mn is observed (Fig. 6d), suggesting that Zoo-rez-2 contains less detrital material. This is supported by the observed lowest amounts of Al and Mn of all tracks. Therefore, P and Y cannot be considered as pure proxies for soil activity/precipitation, but also for detrital input. However, the detrital input seams not to be regular as the input of humic particles. This is determined by the results of the fluorescence microscopy, where the brownish pigmented layers show a stronger UV-luminescence (Fig. 4b). In the case of detrital input during the flushing phase of the year the brownish-pigmented layers should not show a strong luminescence, because the detrital material appears dark in the UV-luminescence. Furthermore, Mn and Al do not show a seasonal cyclicity, but show very high concentrations in the detrital rich sections at approximately 2 and 15 mm dft confirming their association with detrital material.

Magnesium shows the strongest seasonal cyclicity and is interpret as a proxy for the seasonal recharge cycle. Therefore, we averaged the Mg concentration for each year by wiggle matching the visible annual laminae to the Mg (see section 5.2). The resulting annually resolved Mg series from 1839 to 1970 AD shows a positive correlation of $r = 0.22$ ($p < 0.05$) with the lamina thickness chronology (Fig. 12). This correlation is not only due to the same long-term trend, but also the year to year variability especially in the 20th century show a correlation of $r = 0.26$ ($p < 0.05$) after detrending with a 10 point FFT (Fast Fourier Transformation) filter. Since lamina thickness is also interpreted as a proxy for precipitation (see section 5.3.3), this positive correlation is surprising, in particular as the annual Mg cycle shows a negative correlation to infiltration. However, this positive correlation may be explained as follows: Higher rainfall may induce more active vegetation, which results in higher soil pCO_2 (Harper et al., 2005; Wassenburg et al., 2012; Borsato et al., 2015). This CO_2 is dissolved in the seeping water and may result in an increased dissolution of the hostrock, which in the case of Zoolithencave consist of dolomite. Due to more dissolved ions

Clim. Past Discuss., doi:10.5194/cp-2016-18, 2016
Manuscript under review for journal Clim. Past
Published: 15 February 2016

in the drip water and as well still air filled cavities, more PCP takes place. This results in an increase of both the total amount dissolved Ca^{2+} ions and the Mg/Ca ratio of the drip water. Consequently, during years of higher rainfall, both growth rate and the annual Mg content of the speleothem should increase (Wassenburg et al., 2012). Thus, both growth rate and mean annual Mg concentration should be proxies for past precipitation. The opposite interpretation of the Mg concentration on the seasonal and annual time-scale highlights the complexity of trace element signals in speleothems. A similar phenomenon was also detected by Treble et al. (2003) for Sr.

5.3.2 UV-luminescence

Luminescence in speleothems induced by UV-light has been associated due to humic and fulvic acids, which are transported from the soil zone into the cave via the drip water (McGarry and Baker, 2000; van Beynen et al., 2001; Shopov, 2003). In the UV-microscopy picture, it is obvious that the brownish layers are luminescent, which is due to their higher content of humic and fulvic acids originating from the soil. These layers are formed during autumn and winter, when the organic material produced during the vegetation period is flushed into the cave (Sundqvist et al., 2005; Orland et al., 2012).

The G/B ratios taken with the *Aavatech* core scanner have been interpreted as reflecting the amount of humic acids in corals (Grove et al., 2010). This relationship should generally be also valid for speleothems. Since, Y and P are elevated in the brownish layers (Borsato et al., 2007), a positive correlation between the G/B ratio and these elements should occur. Indeed, Y has been associated with fluorescent laminae in speleothems (Fairchild et al., 2010). This is not the case for the three Zoo-rez stalagmites. The reason for this observation is the inclusion of detrital material in all stalagmites, which shows no or only very low UV-luminescence. This is obvious in the comparison of the G/B ratio with the content of Mn and Y (Fig. 13). The G/B ratio is low when Mn and, therefore, the content of detrital material is high. In some sections Y is positively correlated with the G/B ratio. However, in other sections, containing more detrital material (which may also contain Y), a negative correlation is observed to the G/B ratio. In this case, the humic acid signal in the G/B ratio is overprinted by detrital material. Similarly, the long-term decreasing trend in the G/B ratios of the three Zoo-rez stalagmites results from the higher amount of detrital material in the top sections of the stalagmites and cannot be used as a proxy for past precipitation. In summary, the G/B ratio appears to be not appropriate to detect changes in humic acid content of these speleothems, which contain – at least in some parts – relatively high amounts of detrital material. Furthermore, as discussed previously, the resolution of 70 µm/pixel makes it impossible to detect thinner (i.e., with a thickness < 140 µm) annual laminae.

5.3.3 Lamina thickness

We interpret annual lamina thickness as a proxy for past precipitation. Thus, we correlated the lamina thickness series to instrumental data from the meteorological station Bamberg (www.dwd.de), which provides data from 1949 AD to present. Since stalagmite Zoo-rez stopped growing in 1970 AD, only 22 years of overlapping proxy and instrumental data are available. We found no significant correlation between lamina thickness and surface temperature, neither for the annual mean nor for individual months. In contrast, a positive, but insignificant correlation ($r = 0.33$; $p > 0.05$; $N = 22$) between lamina thickness and annual precipitation was found, as has been reported in other studies (Genty and Quinif, 1996; Proctor et al., 2000). In order to test for a better correlation, the lamina thickness chronology was shifted along the precipitation time series (both back in time and up to 1999 AD, the year when the stalagmites were sampled). The maximum correlation was found, assuming a cessation of stalagmite growth in 1970 AD. This is in good agreement with the dating results (see section 5.1). A probable reason for the three stalagmites to stop growing in 1970 could be that further exploration of the deeper parts of the cave started in 1971. Furthermore, the correlation between precipitation of all individual months of the previous, the current, and the next year and lamina thickness was calculated (cf., Tan et al., 2006). In addition, different seasons were compiled to check whether the correlation increases. This is a standard approach in tree-ring research (e.g., Treydte et al., 2001; Buentgen et al., 2005; Wilson et al., 2005; Konter et al., 2014). The highest correlation for an individual month ($r = 0.64$; $p < 0.001$) is observed for December of the current year and $r = 0.57$ ($p < 0.01$) is observed for the season of previous December and current January, February, March, April, May, and December (DJFMAMD). Most probably the clear layer is formed during January to May and the brownish layer during December. This would also explain the contribution of the previous December, because the boundary from the brownish to the clear layer is not sharp (Fig. 4a) and could be not exactly at the end of one year. This shows that stalagmite growth is dominated by the winter season as expected from the higher amount of recharge during winter

Clim. Past Discuss., doi:10.5194/cp-2016-18, 2016
Manuscript under review for journal Clim. Past
Published: 15 February 2016

(Wackerbarth et al., 2010; Mischel et al., 2015). Furthermore, this proves that the upper limit of the brownish, pigmented layers corresponds to the end of the year.

These results provide the background in order to reconstruct past precipitation further back in time using lamina thickness in speleothems from Zoolithencave. A comparison of the sum of precipitation during DJFMAMD and the lamina thickness series with a precipitation reconstruction based on tree-ring width in the Bavarian forest (Wilson et al., 2005) shows a similar pattern (Fig. 15) further supporting that lamina thickness reflects past precipitation variability. Note that the tree-ring width reconstruction is for spring and summer months (March, April, May, June, July, and August; MAMJJA) and, thus, a different season than our record.

6 Conclusions

1. The arrangement of the three Zoo-rez stalagmites grew from 1800 to 1970 AD, which is supported by the detection of the ^{14}C bomb peak, ^{14}C-dating of a charcoal piece below the stalagmite, and lamina counting.
2. The three stalagmites show three types of annual laminae: visible, UV-luminescent, and elemental laminae.
3. Visible laminae consist of a clear and a brownish pigmented layer pair. Measurements of lamina thickness along five tracks on the three stalagmites results in a cross-dated lamina thickness chronology, which is a proxy for winter and spring (DJFMAMD) precipitation.
4. UV-luminescent laminae correspond to the brownish pigmented layers. Using UV-luminescence scanning, the annual laminae could not be detected due to the minimum resolution of 70 µm/pixel.
5. Elemental laminae are clearly visible in Mg, Ba, and Sr, and are strongest for Mg. All three elements are influenced by PCP, which is higher during spring and summer and lower during autumn and winter.
6. Yttrium and P content are higher in the brownish pigmented layers and induced by an annual flush of humic and fulvic acids, when infiltration increases. Both elements are also incorporated in association with detrital material. Thus, Y and P are no clear precipitation proxies. Manganese and Al are associated with detrital material.

7. A mean curve of the Mg content of all tracks was wiggle matched to the lamina thickness chronology resulting in an annual Mg time series. This correlates positively with the lamina thickness chronology and is also influenced by PCP, which is higher in years with more precipitation due to more active vegetation and therefore, more hostrock dissolution.
8. These results highlights the potential of annually laminated speleothems from Zoolithencave for reconstruction of past precipitation variability.

Acknowledgments

Dana Riechelmann is grateful to the DFG for funding (RI 2136/2-1). We thank the "Forschungsgruppe Höhlen und Karst Franken e.V." for the permission to sample stalagmites from Zoolithencave and support during the cave trip in 1999. For assistance during LA-ICPMS, we thank B. Stoll and U. Weis from MPI for Chemistry, Mainz (MPIC) as well as J. Faust. Furthermore, we thank B. Schwager (MPIC) for support during sample preparation for ^{230}Th/U-dating. UV-Luminescence measurements were supported by B. Koster at the NIOZ. We also thank K. Seelos for scanning the thin sections and M. Veicht for some graphic editing. B. Kromer from the Curt-Engelhorn-Zentrum for Archeometry gGmbH (Mannheim) is thanked for ^{14}C-analyses. Finally, we thanks A. Immenhauser for the possibility to use the UV-fluorescence microscopy facility at the Ruhr-University Bochum.

References

Baker, A., Caseldine, C. J., Gilmour, M. A., Charman, D., Proctor, C. J., Hawkesworth, C. J., and Phillips, N.: Stalagmite luminescence and peat humification records of palaeomoisture for the last 2500 years, Earth and Planetary Science Letters, 165, 157-162, 1999.

Baker, A., Smith, C. L., Jex, C., Fairchild, I. J., Genty, D., and Fuller, L.: Annually laminated speleothems: a review, International Journal of Speleology, 37, 193-206, 2008.

Baker, A., Wilson, R., Fairchild, I. J., Franke, J., Spötl, C., Mattey, D., Trouet, V., and Fuller, L.: High resolution δ^{18}O and δ^{13}C records from an annually laminated Scottish stalagmite and relationship with last millennium climate, Global and Planetary Change, 79, 303-311, 2011.

Bischoff, J. L., and Fitzpatrick, J. A.: U-series dating of impure carbonates: An isochron technique using total-sample dissolution, Geochimica et Cosmochimica Acta, 55, 543-554, 1991.

Boch, R., and Spötl, C.: The origin of lamination in stalagmites from Katerloch Cave, Austria: Towards a seasonality proxy, PAGES News, 16, 21-22, 2008.

Boch, R., Spötl, C., and Frisia, S.: Origin and palaeoenvironmental significance of lamination in stalagmites from Katerloch Cave, Austria, Sedimentology, 58, 508-531, 10.1111/j.1365-3091.2010.01173.x, 2011.

Clim. Past Discuss., doi:10.5194/cp-2016-18, 2016
Manuscript under review for journal Clim. Past
Published: 15 February 2016

Borsato, A., Frisia, S., Fairchild, I. J., Somogyi, A., and Susini, J.: Trace element distribution in annual stalagmite laminae mapped by micrometer-resolution X-ray fluorescence: Implications for incorporation of environmentally significant species, Geochimica et Cosmochimica Acta, 71, 1494-1512, 2007.

Borsato, A., Frisia, S., and Miorandi, R.: Carbon dioxide concentration in temperate climate caves and parent soils over an altitudinal gradient and its influence on speleothem growth and fabrics, Earth Surface Processes and Landforms, 40, 1158-1170, 2015.

Brook, G. A., Rafter, M. A., Railsback, L. B., Sheen, S.-W., and Lundberg, J.: A high-resolution proxy record of rainfall and ENSO since AD 1550 from layering in stalagmites from Anjohibe Cave, Madagascar, The Holocene, 9, 695-705, 1999.

Buentgen, U., Esper, J., Frank, D. C., Nicolussi, K., and Schmidhalter, M.: A 1052-year tree-ring proxy for Alpine summer temperatures, Climate Dynamics, 25, 141-153, 2005.

Büntgen, U., Frank, D., Grudd, H., and Esper, J.: Long-term summer temperature variations in the Pyrenees, Climate Dynamics, 31, 615-631, 2008.

Büntgen, U., Tegel, W., Nicolussi, K., McCormick, M., Frank, D., Trouet, V., Kaplan, J. O., Herzig, F., Heussner, K.-U., Wanner, H., Luterbacher, J., and Esper, J.: 2500 Years of European Climate Variability and Human Susceptibility, Science, 331, 578-582, 10.1126/science.1197175, 2011.

Cheng, H., Edwards, R. L., Hoff, J., Gallup, C. D., Richards, D. A., and Asmerom, Y.: The half-lives of uranium-234 and thorium-230, Chemical Geology, 169, 17-33, 2000.

Diedrich, C.: Holotype skulls, stratigraphy, bone taphonomy and excavation history in the Zoolithen Cave and new theory about Espers's "great deluge", Quaternary Science Journal, 63, 78-98, 2014.

Dreyer, R.: Die Zoolithenhöhle bei Burggaillenreuth (Fränkische Alb): Revisionskartierung und Ereignisabfolge, Bochumer Geologische und Geotechnische Arbeiten, 55, 153-167, 2000.

Esper, J., Frank, D. C., Timonen, M., Zorita, E., Wilson, R. J. S., Luterbacher, J., Holzkamper, S., Fischer, N., Wagner, S., Nievergelt, D., Verstege, A., and Buntgen, U.: Orbital forcing of tree-ring data, Nature Clim. Change, 2, 862-866, 2012.

Esper, J. F.: Ausführliche Nachricht von neuentdeckten Zoolithen unbekannter vierfüsiger Thiere, und denen sie enthaltenen, so wie verschiedenen andern, denkwürdigen Grüften der Obergebürgischen Lande des Marggrafthums Bayreuth, Nürnberg, 148 pp., 1774.

Fairchild, I. J., Tuckwell, G. W., Baker, A., and Tooth, A. F.: Modelling of dripwater hydrology and hydrogeochemistry in a weakly karstified aquifer (Bath, UK): Implications for climate change studies Journal of Hydrology, 321, 213-231, 2006.

Fairchild, I. J., Spötl, C., Frisia, S., Borsato, A., Susini, J., Wynn, P. M., and Cauzid, J.: Petrology and geochemistry of annually laminated stalagmites from an Alpine cave (Obir, Austria): seasonal cave physiology, Geological Society Special Publication, 2010.

Fohlmeister, J., Kromer, B., and Mangini, A.: The Influence of Soil Organic Matter Age Spectrum on the Reconstruction of Atmospheric ^{14}C Levels via Stalagmites, Radiocarbon, 53, 99-115, 2011.

Friedrich, M., Remmele, S., Kromer, B., Hofmann, J., Spurk, M., Kauser, K. F., Orcel, C., and Kuppers, M.: The 12,460-year Hohenheim oak and pine tree-ring chronology from Central Europe; a unique annual record for radiocarbon calibration and paleoenvironment reconstructions, Radiocarbon, 46, 1111-1122, 2004.

Frisia, S., Borsato, A., Preto, N., and McDermott, F.: Late Holocene annual growth in three Alpine stalagmites records the influence of solar activity and the North Atlantic Oscillation on winter climate, Earth and Planetary Science Letters, 216, 411-424, 2003.

Frisia, S.: Microstratigraphic logging of calcite fabrics in speleothems as tool for palaeocliamte studies, International Journal of Speleology, 44, 1-16, 2015.

Clim. Past Discuss., doi:10.5194/cp-2016-18, 2016
Manuscript under review for journal Clim. Past
Published: 15 February 2016

Fritts, H. C.: Tree Rings and Climate, The Blackburn Press, Caldwell, New Yersey, 567 pp., 1976.

Genty, D., and Quinif, Y.: Annually laminated sequences in the internal structure of some Belgian stalagmites - importance for paleoclimatology, Journal of Sedimentary Research, 66, 275-288, 1996.

Groiß, J. T.: Geologische und paläontologische Untersuchungen in der Zoolithenhöhle, Geologische Blätter für Nordost.Bayern und angrenzende Gebiete, 29, 26-49, 1979.

Groiß, J. T.: Das Pleistozän in Franken, Karst und Höhle, 105-115, 1988.

Grove, C. A., Nagtegaal, R., Zinke, J., Scheufen, T., Koster, B., Kasper, S., McCulloch, M. T., van den Bergh, G., and Brummer, G. J. A.: River runoff reconstructions from novel spectral luminescence scanning of massive coral skeletons, Coral Reefs, 29, 579-591, 2010.

Hammer, O., Harper, D. A. T., and Ryan, P. D.: PAST: Paleontological statistics software package for education and data analysis, Palaeontologia Electronica, 4, 9pp., 2001.

Hardt, B., Rowe, H. D., Springer, G. S., Cheng, H., and Edwards, R. L.: The seasonality of east central North American precipitation based on three coeval Holocene speleothems from southern West Virginia, Earth and Planetary Science Letters, 295, 342-348, 2010.

Harper, C. W., Blair, J. M., Fay, P. A., Knapp, A. K., and Carlisle, J. D.: Increased rainfall variability and reduced rainfall amount decreases soil CO_2 flux in a grassland ecosystem, Global Change Biology, 11, 322-334, 2005.

Holmes, R. L.: Computer-assisted quality control in tree-ring dating and measurment, Tree-Ring Bulletin, 43, 69-78, 1983.

Hua, Q., Barbetti, M., and Rakowski, A. Z.: Atmospheric Radiocarbon for the period 1950-2010, Radiocarbon, 55, 2059-2072, 2013.

Huang, Y. M., Fairchild, I. J., Borsato, A., Frisia, S., Cassidy, N. J., McDermott, F., and Hawkesworth, C. J.: Seasonal variations in Sr, Mg, and P in modern speleothems (Grotta di Ernesto, Italy), Chemical Geology, 175, 429-448, 2001.

Jochum, K. P., Weis, U., Stoll, B., Kuzmin, D., Yang, Q., Raczek, I., Jacob, D. E., Stracke, A., Birbaum, K., Frick, D. A., Günther, D., and Enzweiler, J.: Determination of Reference Values for NIST SRM 610–617 Glasses Following ISO Guidelines, Geostandards and Geoanalytical Research, 35, 397-429, 2011.

Johnson, K. R., Hu, C., Belshaw, N. S., and Henderson, G. M.: Seasonal trace-element and stable-isotope variations in a Chinese speleothem: The potential for high-resolution paleomonsoon reconstruction, Earth and Planetary Science Letters, 244, 394-407, 2006.

Kaufman, A.: An evaluation of several methods for determining ^{230}ThU ages in impure carbonates, Geochimica et Cosmochimica Acta, 57, 2303-2317, 1993.

Kennett, D. J., Breitenbach, S. F. M., Aquino, V. V., Asmerom, Y., Awe, J., Baldini, J. U. L., Bartlein, P., Culleton, B. J., Ebert, C., Jazwa, C., Macri, M. J., Marwan, N., Polyak, V., Prufer, K. M., Ridley, H. E., Sodemann, H., Winterhalder, B., and Haug, G. H.: Development and Disintegration of Maya Political Systems in Response to Climate Change, Science, 338, 788-791, 10.1126/science.1226299, 2012.

Konter, O., Holzkämper, S., Helle, G., Büntgen, U., Saurer, M., and Esper, J.: Climate sensitivity and parameter coherency in annually resolved Î´13C and Î´18O from Pinus uncinata tree-ring data in the Spanish Pyrenees, Chemical Geology, 377, 12-19, 2014.

Ku, T.-L., and Liang, Z.-C.: The dating of impure carbonates with decay-series isotopes, Nuclear Instruments and Methods in Physics Research, 223, 563-571, 1984.

Mattey, D., Lowry, D., Duffet, J., Fisher, R., Hodge, E., and Frisia, S.: A 53 year seasonally resolved oxygen and carbon isotope record from a modern Gibraltar speleothem: Reconstructed drip water and relationship to local precipitation, Earth and Planetary Science Letters, 269, 80-95, 2008.

Clim. Past Discuss., doi:10.5194/cp-2016-18, 2016
Manuscript under review for journal Clim. Past
Published: 15 February 2016

McGarry, S. F., and Baker, A.: Organic acid fluorescence:applications to speleothem palaeoenvironmental reconstruction, Quaternary Science Reviews, 19, 1087-1101, 2000.

Meyer, F. T.: Three year monitoring in caves of the Northern Franconian Alb - Data, Analysis and Discussion, Master of Science, Institute of Geology, Mineralogy and Geophysics, Ruhr-University Bochum, Bochum, 57 pp., 2014.

Meyer, R. K. F.: Stratigraphie und Fazies des Frankendolomits (Malm), Erlanger geologische Abhandlungen, Geologisches Inst., Erlangen, 28 pp., 1972.

Mischel, S., Scholz, D., and Spötl, C.: $\delta^{18}O$ values of cave drip water: a promising proxy for the reconstruction of the North Atlantic Oscillation?, Climate Dynamics, 1-16, 2015.

Myers, C. G., Oster, J. L., Sharp, W. D., Bennartz, R., Kelley, N. P., Covey, A. K., and Breitenbach, S. F. M. C. G. L.: Northeast Indian stalagmite records Pacific decadal climate change: Implications for moisture transport and drought in India, Geophysical Research Letters, 42, 4124-4132, 2015.

Navarra, A., and Simoncini, V.: A Data Analysis Guide to Empirical Orthogonal Functions for Climate, Springer, Dordrecht, Heidelberg, London, New York, 2010.

Noronha, A. L., Johnson, K. R., Southon, J. R., Hu, C., Ruan, J., and McCabe-Glynn, S.: Radiocarbon evidence for decomposition of aged organic matter in the vadose zone as the main source of speleothem carbon, Quaternary Science Reviews, 127, 37-47, 2015.

Obert, J. C., Scholz, D., Felis, T., Brocas, W., Jochum, K. P., and Andreae, M. O.: $^{230}Th/U$ dating of Last Interglacial brain corals from Bonaire (southern Caribbean) using bulk and theca wall material, Geochimica et Cosmochimica Acta, accepted.

Orland, I. J., Bar-Matthews, M., Ayalon, A., Matthews, A., Kozdon, R., Ushikubo, T., and Valley, J. W.: Seasonal resolution of Eastern Mediterranean climate change since 34 ka from a Soreq Cave speleothem, Geochimica et Cosmochimica Acta, 89, 240-255, 2012.

Paillard, D., Labeyrie, L., and Yiou, P.: AnalySeries 1.0: aMacintosh sofware for the analysis of geophysical time-series., EOS, 77, 379, 1996.

Pons-Branchu, E., Douville, E., Roy-Barman, M., Dumont, E., Branchu, P., Thil, F. o., Frank, N., Bordier, L., and Borst, W.: A geochemical perspective on Parisian urban history based on U-Th dating, laminae counting and yttrium and REE concentrations of recent carbonates in underground aqueducts, Quaternary Geochronology, 24, 44-53, 2014.

Proctor, C. J., Baker, A., Barnes, W. L., and Gilmour, M. A.: A thousand year speleothem proxy record of North Atlantic climate from Scotland, Climate Dynamics, 16, 815-820, 2000.

Proctor, C. P., Baker, A. B., and Barnes, W. B.: A three thousand year record of North Atlantic climate, Climate Dynamics, 19, 449-454, 10.1007/s00382-002-0236-x, 2002.

Przybylowicz, W., Schwarcz, H. P., and Latham, A. G.: Dirty calcites 2. Uranium-series dating of artificial calcite-detritus mixtures, Chemical Geology: Isotope Geoscience section, 86, 161-178, 1991.

Railsback, L. B., Brook, G. A., Chen, J., Kalin, R., and Fleisher, C. J.: Environmental controls on the petrology of late holocene speleothem from Botswana with annual layers of aragonite and calcite, Journal of Sedimentary Research, A64, 147-155, 1994.

Reimer, P. J., Bard, E., Bayliss, A., Beck, J. W., Blackwell, P. G., Bronk Ramsey, C., Buck, C. E., Cheng, H., Edwards, R. L., Friedrich, M., Grootes, P. M., Guilderson, T. P., Haflidason, H., Hajdas, I., Hatté, C., Heaton, T. J., Hoffmann, D. L., Hogg, A. G., Hughen, K. A., Kaiser, K. F., Kromer, B., Manning, S. W., Niu, M., Reimer, R. W., Richards, D. A., Scott, E. M., Southon, J. R., Staff, R. A., Turney, C. S. M., and van der Plicht, J.: IntCal13 and Marine13 Radiocarbon Age Calibration Curves 0-50,000 Years cal BP, Radiocarbon, 55, 1869-1887, 2013.

Richards, D. A., and Dorale, J. A.: Uranium-series Chronology and Environmental Applications of Speleothems, Reviews in Mineralogy and Geochemistry, 52, 407-460, 2003.

Richter, D. K., Neuser, R. D., Schreuer, J., Gies, H., and Immenhauser, A.: Radiaxial-fibrous calcites: A new look at an old problem, Sedimentary Geology, 239, 23-36, 2011.
Richter, D. K., Harder, M., Niedermayr, A., and Scholz, D.: Zopfsinter in der Zoolithenhöhle: Erstfund kryogener Calcite in der Fränkischen Alb, Mitteilungen des Verbandes der deutschen Höhlen- und Karstforscher, 60, 36-41, 2014.
Ridley, H. E., Asmerom, Y., Baldini, J. U. L., Breitenbach, S. F. M., Aquino, V. V., Prufer, K. M., Culleton, B. J., Polyak, V., Lechleitner, F. A., Kennett, D. J., Zhang, M., Marwan, N., Macpherson, C. G., Baldini, L. M., Xiao, T., Peterkin, J. L., Awe, J., and Haug, G. H.: Aerosol forcing of the position of the intertropical convergence zone since ad 1550, Nature Geosci, 8, 195-200, 2015.
Riechelmann, S., Schröder-Ritzrau, A., Wassenburg, J. A., Schreuer, J., Richter, D. K., Riechelmann, D. F. C., Terente, M., Constantin, S., Mangini, A., and Immenhauser, A.: Physicochemical characteristics of drip waters: Influence on mineralogy and crystal morphology of recent cave carbonate precipitates, Geochimica et Cosmochimica Acta, 145, 13-29, 2014.
Roberts, M. S., Smart, P. L., and Baker, A.: Annual trace element variations in a Holocene speleothem, Earth and Planetary Science Letters, 154, 237-246, 1998.
Rosendahl, W.: Neue Erkenntnisse zur Vorgeschichte der Zoolithenhöhle bei Burggaillenreuth, Nordliche Frankenalb, Süddeutschland, Die Höhle, 56, 24-28, 2005.
Rosenmüller, J. C.: Quaedam de ossibus fossilibus animalis cajusdam, historiam ejus et cognitionem accuratiorem illustrantia, dissertatio, quam d. 22. Octob. 1794. ad disputandum proposuit Ioannes Christ. Rosenmüller Heßberga-Francus, LL. AA. M. in Theatro anatomico Lipsiensi Prosector assumto socio Io. Chr. Aug. Heinroth Lips. Med. Stud. Cum tabula aenea, 34, 1794.
Scholz, D., and Hoffmann, D. L.: ^{230}Th/U-dating of fossil reef corals and Speleothems, Quaternary Science Journal (Eiszeitalter und Gegenwart), 57, 52-77, 2008.
Scholz, D., Frisia, S., Borsato, A., Spötl, C., Fohlmeister, J., Mudelsee, M., Miorandi, R., and Mangini, A.: Holocene climate variability in north-eastern Italy: potential influence of the NAO and solar activity recorded by speleothem data, Climate of the Past, 8, 1367-1383, 2012.
Schwarcz, H. P.: Uranium series dating of Quaternary deposits, Quaternary International, 1, 7-17, 1989.
Schwarcz, H. P., and Latham, A. G.: Dirty calcites 1. Uranium-series dating of contaminated calcite using leachates alone, Chemical Geology: Isotope Geoscience section, 80, 35-43, 1989.
Schweingruber, F. H.: Der Jahrring. Standort, Methodik, Zeit und Klima in der Dendrochronologie, Paul Haupt, Bern, 1983.
Shen, C.-C., Lin, K., Duan, W., Jiang, X., Partin, J. W., Edwards, R. L., Cheng, H., and Tan, M.: Testing the annual nature of speleothem banding, Sci. Rep., 3, 2013.
Shopov, Y. Y.: Luminescence of Speleothems, Studi Trentini di Scienze Naturali Acta geologica, 80, 95-104, 2003.
Smith, C. L., Fairchild, I. J., Spötl, C., Frisia, S., Borsato, A., Moreton, S. G., and Wynn, P. M.: Chronology building using objective identification of annual signals in trace element profiles of stalagmites, Quaternary Geochronology, 4, 11-21, 2009.
Speer, J. H.: Fundamentals of Tree-Ring Research, The University of Arizona Press, Tucson, 333 pp., 2010.
Spurk, M., Leuschner, H. H., Baillie, M. G. L., Briffa, K. R., and Friedrich, M.: Depositional frequency of German subfossil oaks: climatically and non-climatically induced fluctuations in the Holocene, The Holocene, 12, 707-715, 10.1191/0959683602hl583rp, 2002.
Sundqvist, H. S., Baker, A., and Holmgren, K.: Luminescence variations in fast-growing stalagmites from Uppsala, Sweden, Geografiska Annaler, 87, 539-548, 2005.

Clim. Past Discuss., doi:10.5194/cp-2016-18, 2016
Manuscript under review for journal Clim. Past
Published: 15 February 2016

Synal, H.-A., Stocker, M., and Suter, M.: MICADAS: A new compact radiocarbon AMS system, Nuclear Instruments and Methods in Physics Research Section B: Beam Interactions with Materials and Atoms, 259, 7-13, 2007.

Tan, M., Baker, A., Genty, D., Smith, C., Esper, J., and Cai, B.: Applications of stalagmite laminae to paleoclimate reconstructions: Comparison with dendrochronology / climatology, Quaternary Science Reviews, 25, 2103-2117, 2006.

Team, R. C.: A Language and Environment for Statistical Computing, edited by: Computing, R. F. f. S., Vienna, Austria, 2015.

Tietz, G. F.: Zur Genese rezenter Karbonatbildungen in Dolomithöhlen Frankens, in: Beiträge zur Karst- und Höhlenforschung in Franken, Karst und Höhle, Verband der deutschen Höhlen- und Karstforscher e.V., Münschen, 7-79, 1988.

Treble, P., Shelley, J. M. G., and Chappell, J.: Comparison of high resolution sub-annual records of trace elements in a modern (1911-1992) speleothem with instrumental climate data from southwest Australia, Earth and Planetary Science Letters, 216, 141-153, 2003.

Treydte, K., Schleser, G. H., Schweingruber, F. H., and Winiger, M.: The climatic significance of δ13C in subalpine spruces (Lötschental, Swiss Alps), Tellus B, 53, 593-611, 10.1034/j.1600-0889.2001.530505.x, 2001.

Trouet, V., Esper, J., Graham, N. E., Baker, A., Scourse, J. D., and Frank, D. C.: Persistent positive North Atlantic Oscilation Mode dominated the Medieval Climate Anomaly, Science, 324, 78-80, 2009.

van Beynen, P., Bourbonniere, R., Ford, D. C., and Schwarcz, H. P.: Cause of colour and fluorescence in speleothems, Chemical Geology, 175, 319-341, 2001.

Van Rampelbergh, M., Verheyden, S., Allan, M., Quinif, Y., Keppens, E., and Claeys, P.: Monitoring of a fast-growing speleothem site from the Han-sur-Lesse cave, Belgium, indicates equilibrium deposition of the seasonal $d^{18}O$ and $d^{13}C$ signals in the calcite, Climate of the Past, 10, 1871-1885, 2014.

von Storch, H., and Zwiers, F. W.: Statistical Analysis in Climate Research, Cambridge University Press, 293 pp., 2002.

Wackerbarth, A., Scholz, D., Fohlmeister, J., and Mangini, A.: Modelling the d18O value of cave drip water and speleothem calcite, Earth and Planetary Science Letters, 299, 387-397, 2010.

Wassenburg, J. A., Immenhauser, A., Richter, D. K., Jochum, K. P., Fietzke, J., Deininger, M., Goos, M., Scholz, D., and Sabaoui, A.: Climate and cave control on Pleistocene/Holocene calcite-to-aragonite transitions in speleothems from Morocco: Elemental and isotopic evidence, Geochimica et Cosmochimica Acta, 92, 23-47, 2012.

Wedepohl, H. K.: The composition of the continental crust, Geochimica et Cosmochimica Acta, 59, 1217-1232, 1995.

Wenz, S., Scholz, D., Sürmelihindi, G., Passchier, C. W., Jochum, K. P., and Andreae, M. O.: ^{230}Th/U-dating of carbonate deposits from ancient aqueducts, Quaternary Geochronology, in review.

Wilson, R. J. S., Luckman, B. H., and Esper, J.: A 500 year dendroclimatic reconstruction of spring–summer precipitation from the lower Bavarian Forest region, Germany, International Journal of Climatology, 25, 611-630, 10.1002/joc.1150, 2005.

Wurth, G., Niggemann, S., and Richter, D. K.: Der hierarchische Aufbau des Laminationsgefüges eines spät/postglazialen Kerzenstalagmiten aus der Zoolithenhöhle bei Burggaillenreuth (Fränkische Schweiz), Bochumer Geologische und Geotechnische Arbeiten, 55, 131-151, 2000.

Wurth, G.: Klimagesteuerte Rhythmik in spät- bis postglazialen Stalagmiten des Sauerlandes, der Fränkischen Alb und der Bayerischen Alpen, Doktor der Naturwissenschaften, Fakultät für Geowissenschaften, Ruhr-Universität Bochum, Bochum, 123 pp., 2002.

Yang, Q., Scholz, D., Jochum, K. P., Hoffmann, D. L., Stoll, B., Weis, U., Schwager, B., and Andreae, M. O.: Lead isotope variability in speleothems - A promising new proxy for hydrological change? First results from a stalagmite from western Germany, Chemical Geology, 396, 143-151, 2015.

Table 1. Results of ^{230}Th/U-dating. All errors are given at the 2σ-level.

Sample	**dft**	**^{238}U [µg/g]**	**$^{234/238}$U**	**^{230}Th/^{238}U**	**$^{230/232}$Th**	**Age uncorr. [ka]**	**Age corr. [ka]**
Zoo-rez-1-o	0.1-0.6 cm	0.0351 ±0.0002	1.1686 ±0.0046	0.0695 ±0.0016	2.6 ±0.1	6.6822 ±0.1629	4.6699 ±0.9998
Zoo-rez-1-u	1.2-1.7 cm	0.0233 ±0.0001	1.1881 ±0.0052	0.0639 ±0.0031	0.9 ±0.04	6.0255 ±0.2985	0.3402 +3.3143 -0.2947

Clim. Past Discuss., doi:10.5194/cp-2016-18, 2016
Manuscript under review for journal Clim. Past
Published: 15 February 2016

Table 2. Results of ^{14}C-dating of charcoal and carbonate.

Sample	**Age [a] refer to 1950 AD**	**δ^{13}C [‰]**	**^{14}C-activity [pmC]**	**Cal 1σ**
Zoo-rez-1, 0.8 mm dft	-1,440 ± 22	-10.5 ± 0.3	119.6287 ± 0.32494	
Zoo-rez-1, 2.2 mm dft	-527 ± 22	-8.6 ± 0.3	106.7865 ± 0.297579	
Zoo-rez-1, 6.9 mm dft	740 ± 24	-7,4 ± 0.3	91.19406 ± 0.275865	
Zoo-rez-2, charcoal	165 ± 21	-23.0 ± 2		AD 1671-1951

Clim. Past Discuss., doi:10.5194/cp-2016-18, 2016
Manuscript under review for journal Clim. Past
Published: 15 February 2016

Climate of the Past Discussions

Table 3. Correlation coefficients calculated between the different elemental concentrations of the individual tracks. a) Zoo-rez-1.1, b) Zoo-rez-1.2, c) Zoo-rez-1.3, d) Zoo-rez-2, e) Zoo-rez-3. Correlation coefficients, r > 0.25 are marked in green, r > 0.5 in orange, and r > 0.7 in red. Negative correlation coefficients, r < -0.3 are marked in blue. All coloured correlations have p values < 0.001.

a)	Mg	Al	P	Mn	Sr	Y
Mg						
Al	0.10					
P	0.07	**0.25**				
Mn	0.22	**0.45**	**0.47**			
Sr	0.19	0.03	-0.01	0.14		
Y	-0.13	0.24	**0.32**	**0.44**	0.01	
Ba	**0.32**	0.05	0.04	0.14	**0.30**	0.06

b)	Mg	Al	P	Mn	Sr	Y
Mg						
Al	0.12					
P	0.14	0.21				
Mn	0.18	**0.31**	**0.65**			
Sr	0.16	-0.01	-0.03	0.02		
Y	0.07	0.07	**0.52**	**0.51**	0.07	
Ba	0.19	0.02	0.04	0.06	0.18	0.10

c)	Mg	Al	P	Mn	Sr	Y
Mg						
Al	0.22					
P	0.12	**0.26**				
Mn	0.23	**0.45**	**0.78**			
Sr	0.19	0.02	-0.01	0.02		
Y	0.02	**0.26**	**0.68**	**0.72**	0.04	
Ba	**0.35**	0.07	0.12	0.17	**0.27**	0.16

d)	Mg	Al	P	Mn	Sr	Y
Mg						
Al	0.09					
P	-0.09	0.23				
Mn	0.18	**0.26**	**0.28**			
Sr	**0.33**	0.01	-0.07	0.03		
Y	**-0.46**	0.06	**0.47**	-0.02	-0.17	
Ba	**0.63**	0.17	0.09	0.13	**0.40**	-0.10

e)	Mg	Al	P	Mn	Sr	Y
Mg						
Al	0.10					
P	0.09	0.13				
Mn	0.14	0.24	**0.34**			
Sr	0.17	-0.03	-0.03	0.05		
Y	-0.12	0.09	**0.45**	0.22	-0.06	
Ba	**0.51**	0.08	0.21	0.24	0.18	0.11

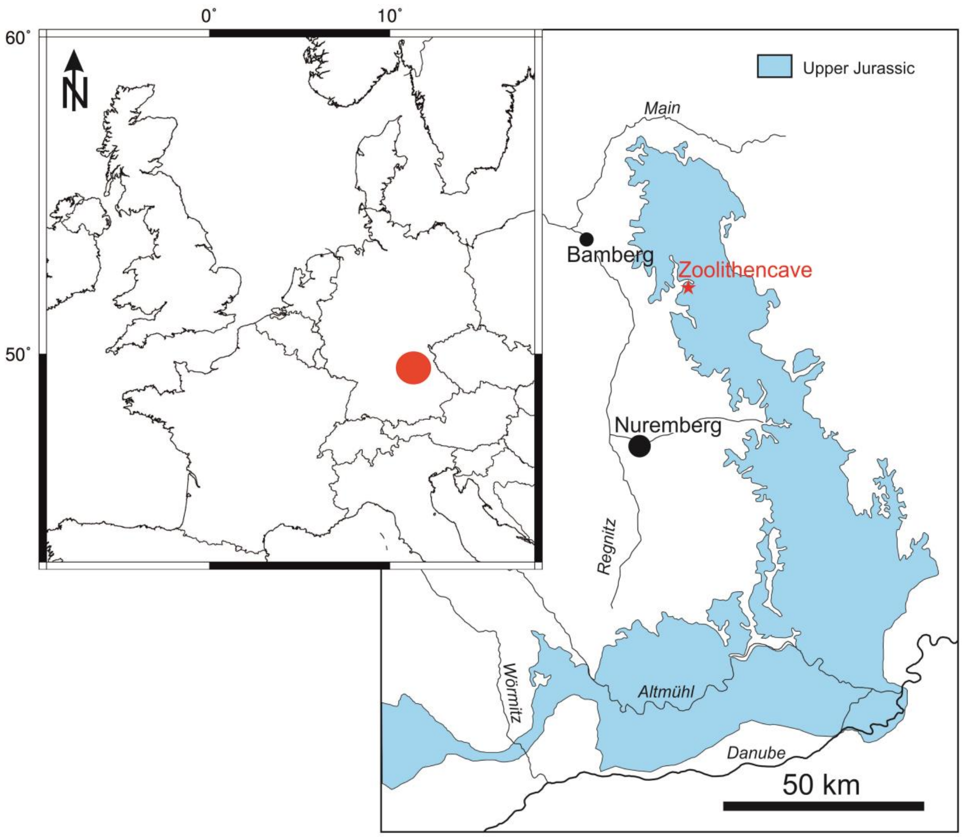

Figure 1. Map of the Upper Jurassic containing marl, limestone, and dolomite (modified after Groiß, 1988). The location of Zoolithencave is indicated by the red star. Location of the region is marked in the map of Central Europe in the upper left.

Clim. Past Discuss., doi:10.5194/cp-2016-18, 2016
Manuscript under review for journal Clim. Past
Published: 15 February 2016

Climate of the Past Discussions

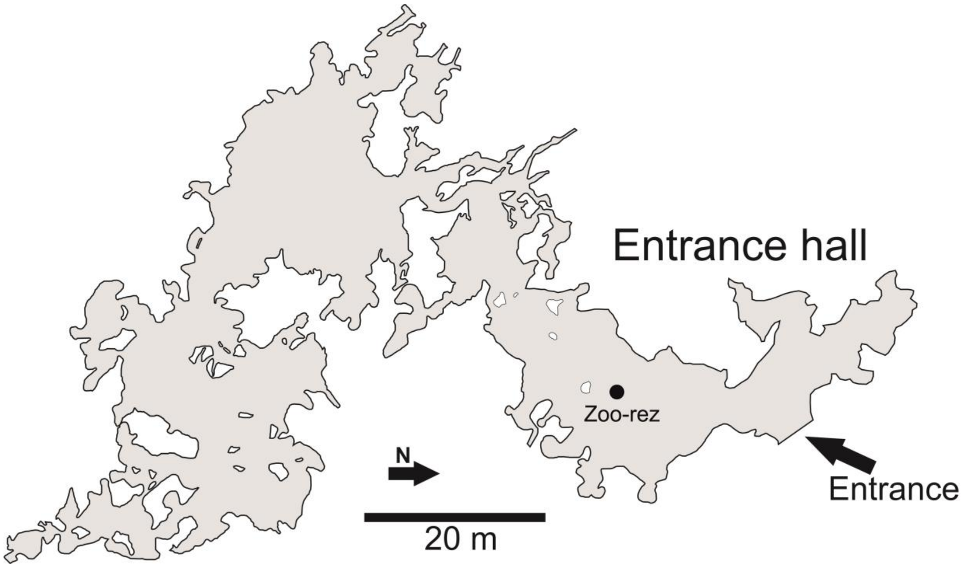

Figure 2. Map of Zoolithencave with the sampling site of Zoo-rez indicated (modified after Dreyer, 2000).

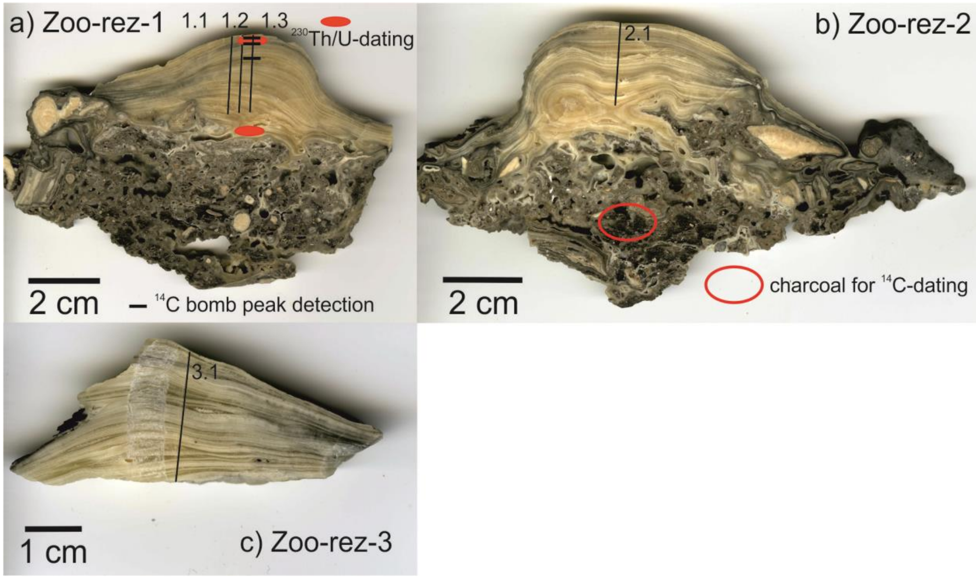

Figure 3. Pictures of the sampling slices of Zoo-rez-1 (a), Zoo-rez-2 (b), and Zoo-rez-3 (c) subsequent to cutting. The laser ablation tracks (labelled 1.1, 1.2, 1.3, 2.1, and 3.1, respectively), the sampling positions for ^{14}C bomb peak detection as well as $^{230}Th/U$-dating, and the charcoal used for ^{14}C-dating are indicated.

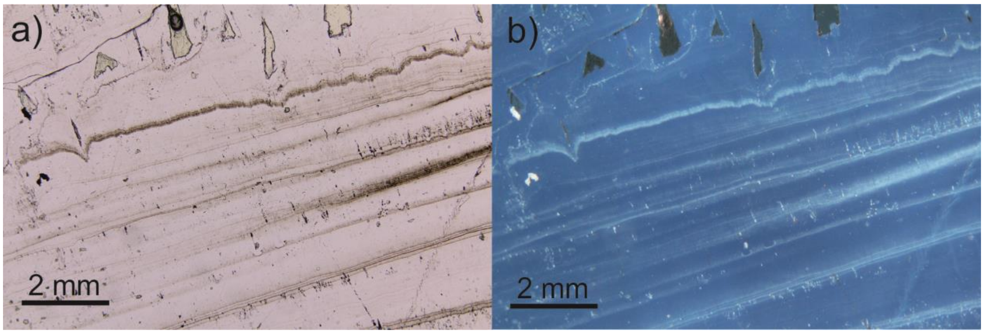

Figure 4. a) Visible laminae in Zoo-rez. Which is present as layer pairs consisting of a clear and a brownish pigmented layer. b) Fluorescence is stronger for the brownish pigmented layers than for the clear layers.

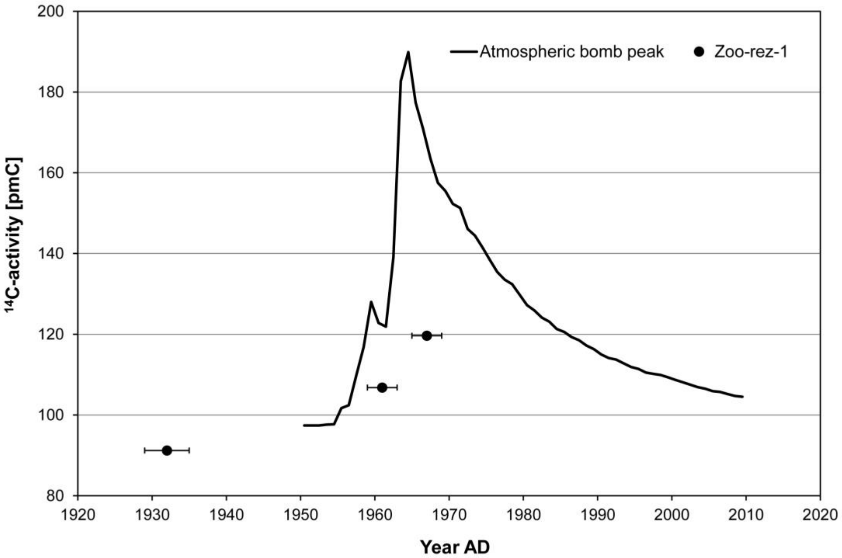

Figure 5. ^{14}C-activity determined for three samples from the top section of Zoo-rez-1 (at 0.8, 2.2, and 6.9 mm dft, respectively) compared with the atmospheric bomb peak (Hua et al., 2013).

Clim. Past Discuss., doi:10.5194/cp-2016-18, 2016
Manuscript under review for journal Clim. Past
Published: 15 February 2016

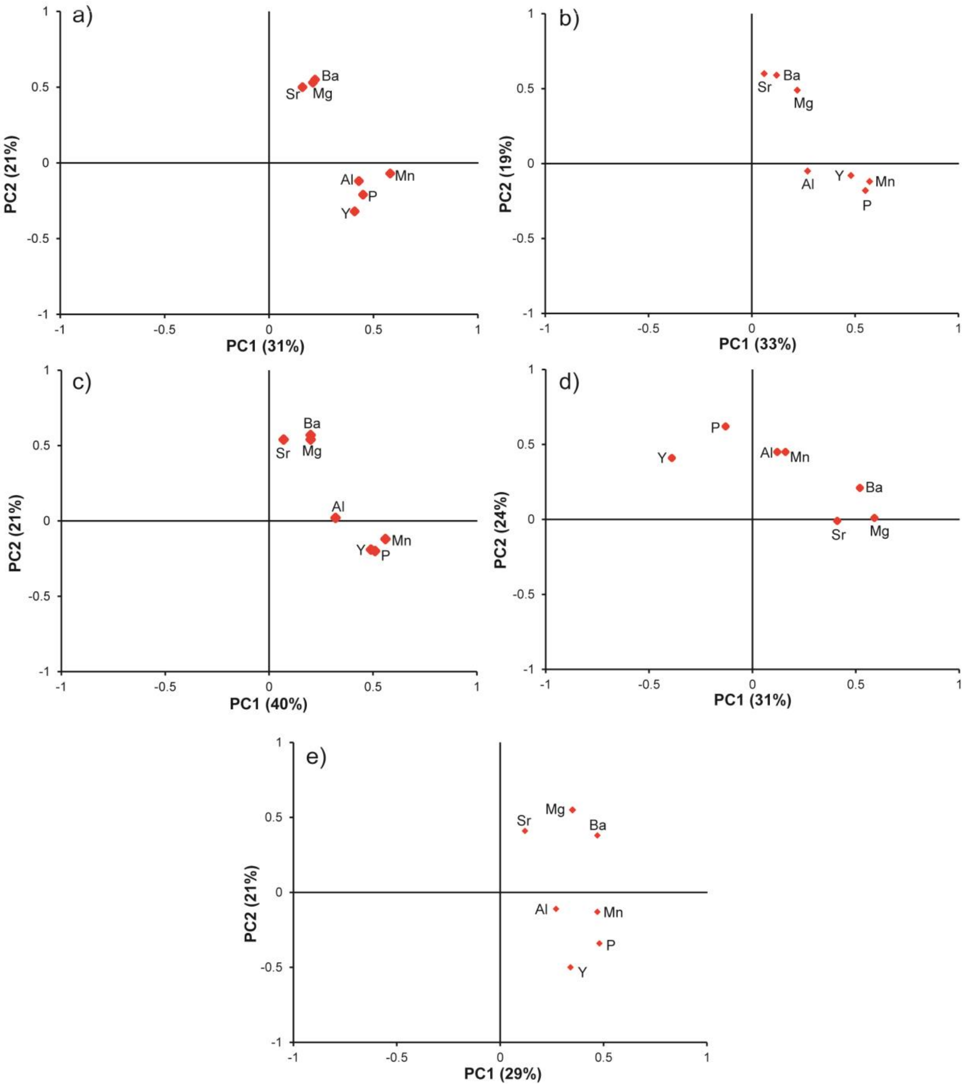

Figure 6. Results of PCA of the element data for the five different tracks. Zoo-rez-1.1 (a), Zoo-rez-1.2 (b), Zoo-rez-1.3 (c), Zoo-rez-2 (d), and Zoo-rez-3 (e).

Clim. Past Discuss., doi:10.5194/cp-2016-18, 2016
Manuscript under review for journal Clim. Past
Published: 15 February 2016

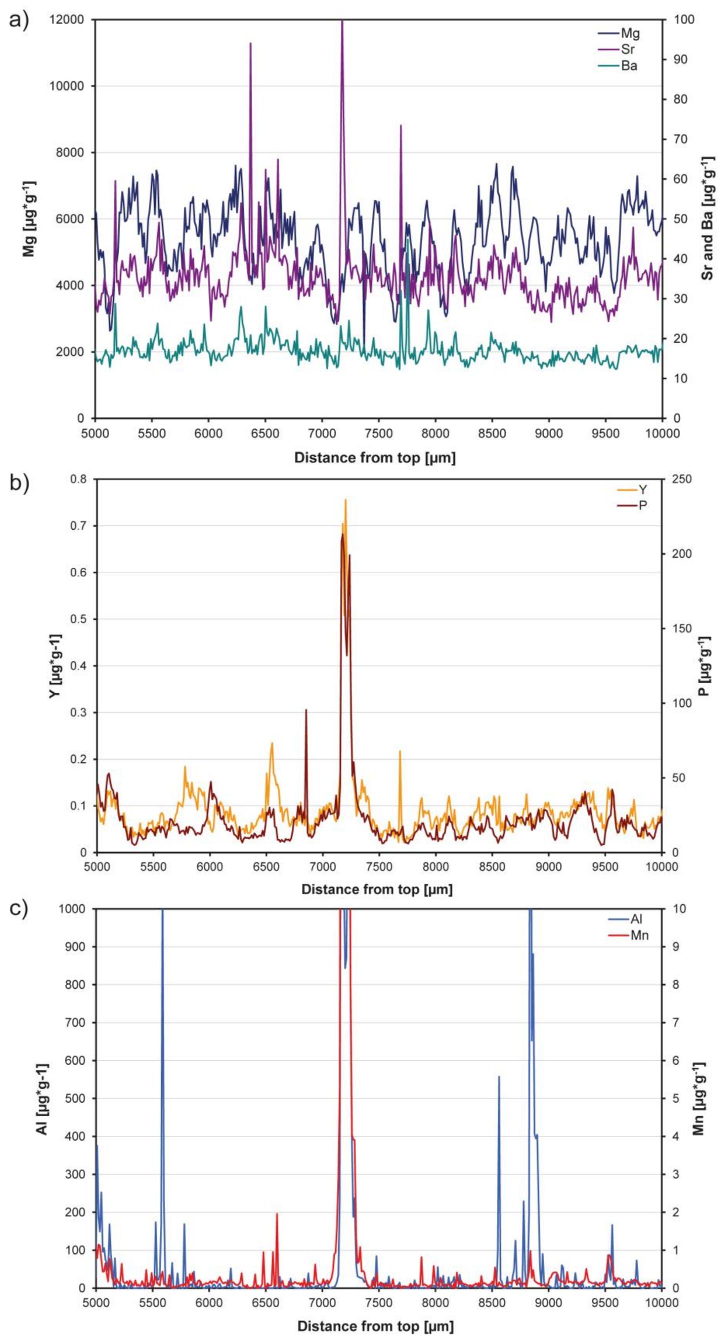

Figure 7. Compilation of Mg, Ba, and Sr (a), Y and P (b), and Al and Mn (c) concentrations in Zoo-rez-1.1 in section 5000 to 10,000 µm dft. The same patterns are observed for Zoo-rez-1.2, 1.3, 2, and 3.

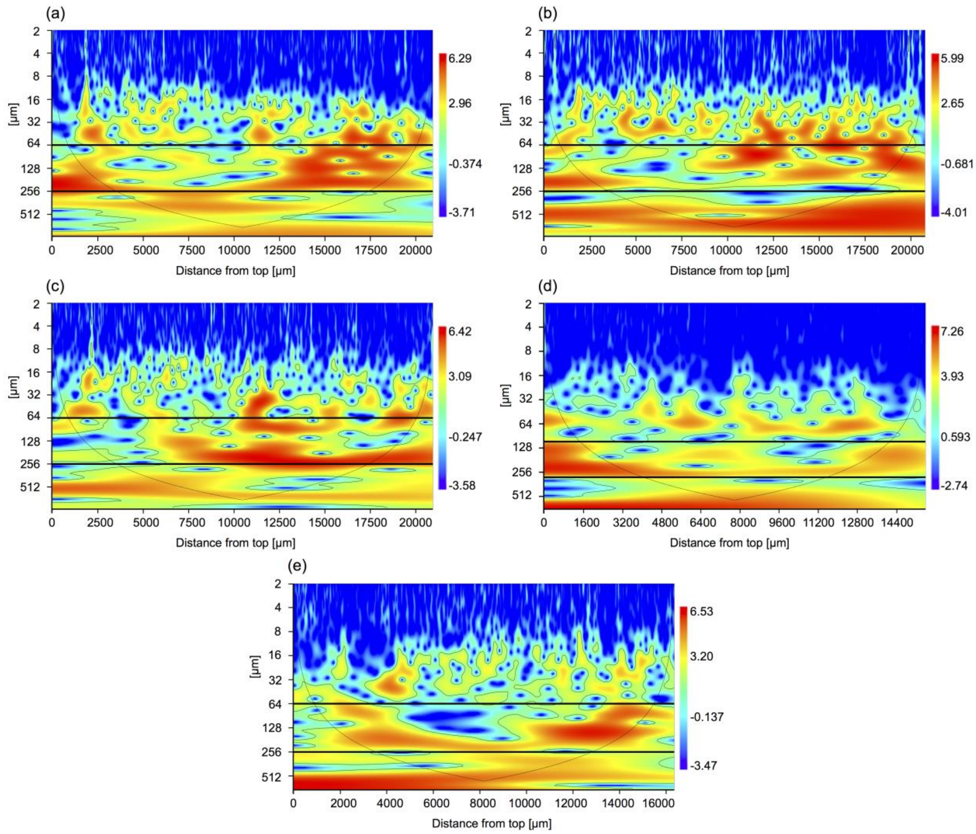

Figure 8. Wavelet analysis of the Mg concentration of the five tracks: Zoo-rez-1.1 (a), Zoo-rez-1.2 (b), Zoo-rez-1.3 (c), Zoo-rez-2 (d), and Zoo-rez-3 (e).

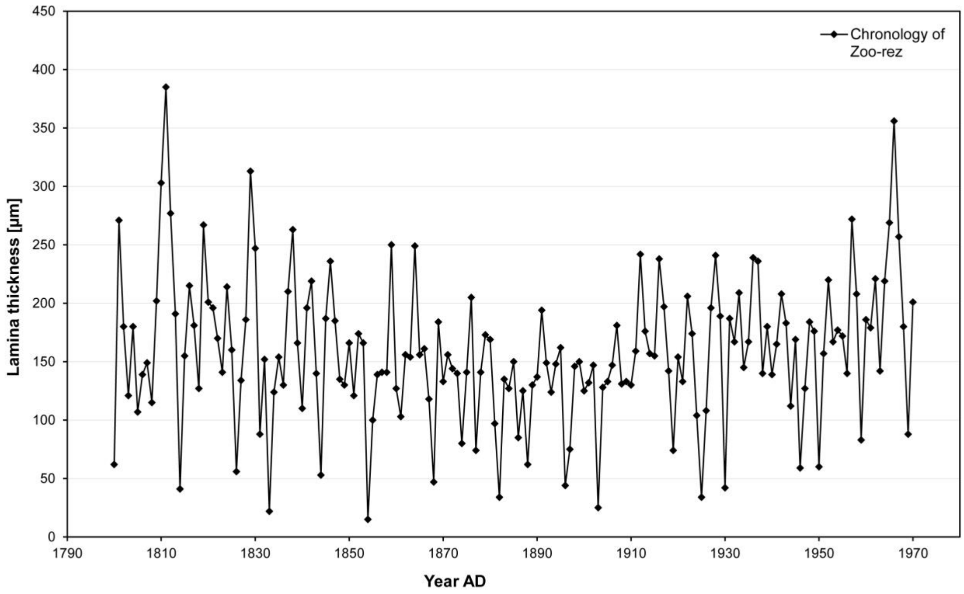

Figure 9. Mean lamina thickness chronology of all five tracks measured on stalagmite Zoo-rez.

Clim. Past Discuss., doi:10.5194/cp-2016-18, 2016
Manuscript under review for journal Clim. Past
Published: 15 February 2016

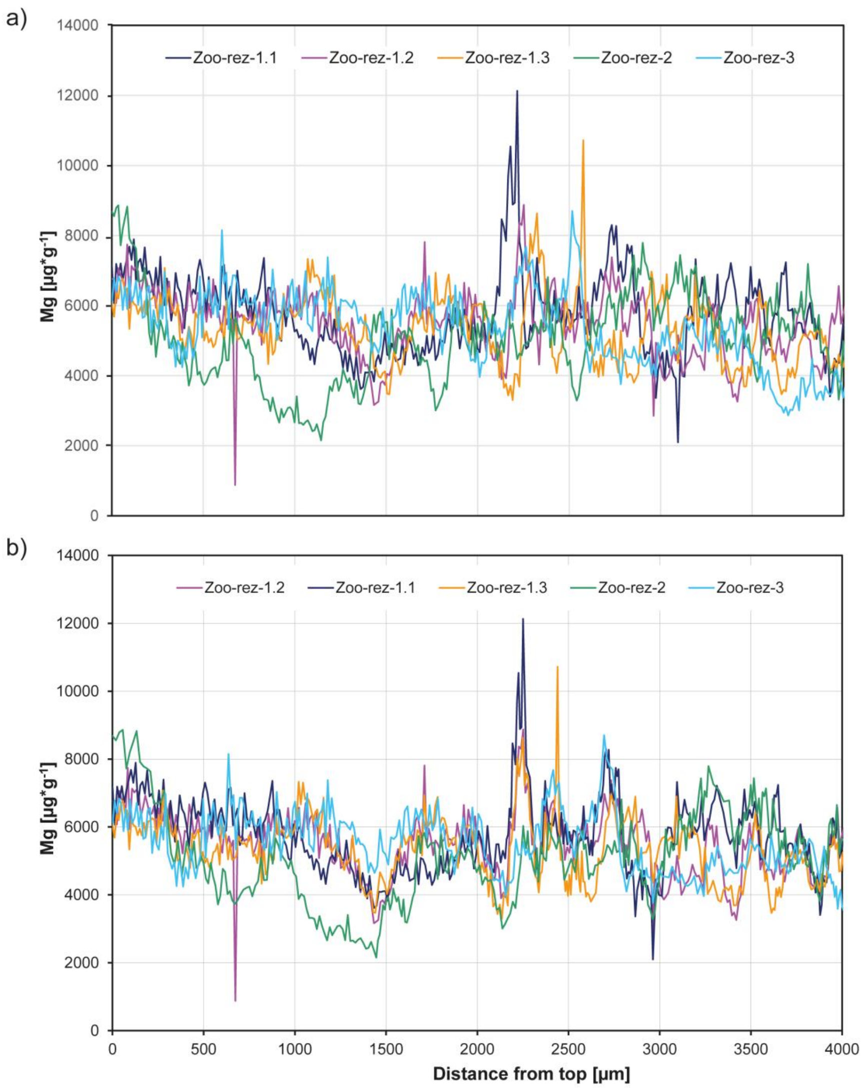

Figure 10. Mg concentration along the five individual tracks on stalagmite Zoo-rez in the section 0 to 4000 µm dft before (a) and after (b) wiggle matching.

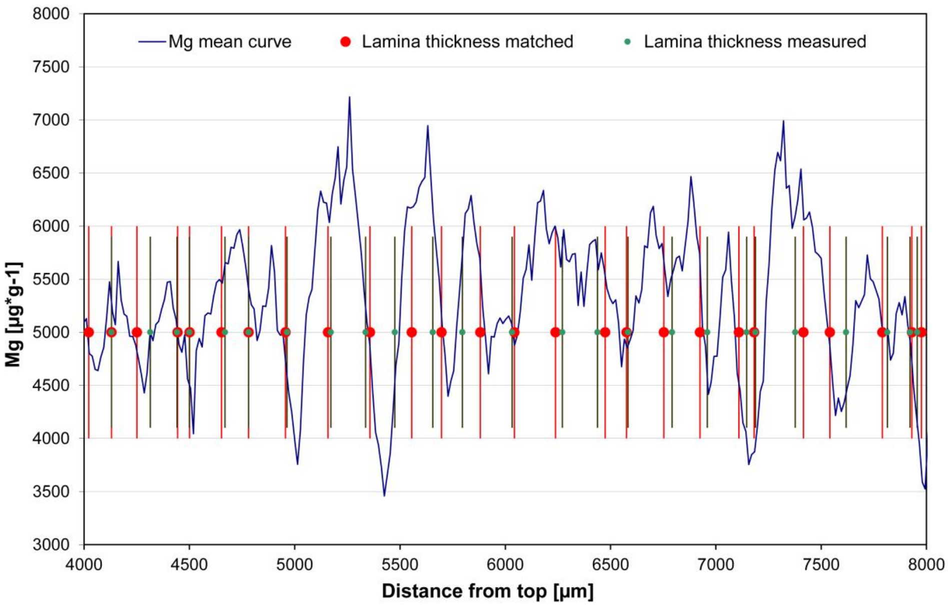

Figure 11. Mean curve of Mg concentration compared with both the matched (red lines) and the measured (green lines) lamina thickness series for the section between 4000 and 8000 µm dft. The boundaries of the lamina were matched to the increase (from bottom to top of the stalagmite) of the Mg concentration.

Clim. Past Discuss., doi:10.5194/cp-2016-18, 2016
Manuscript under review for journal Clim. Past
Published: 15 February 2016

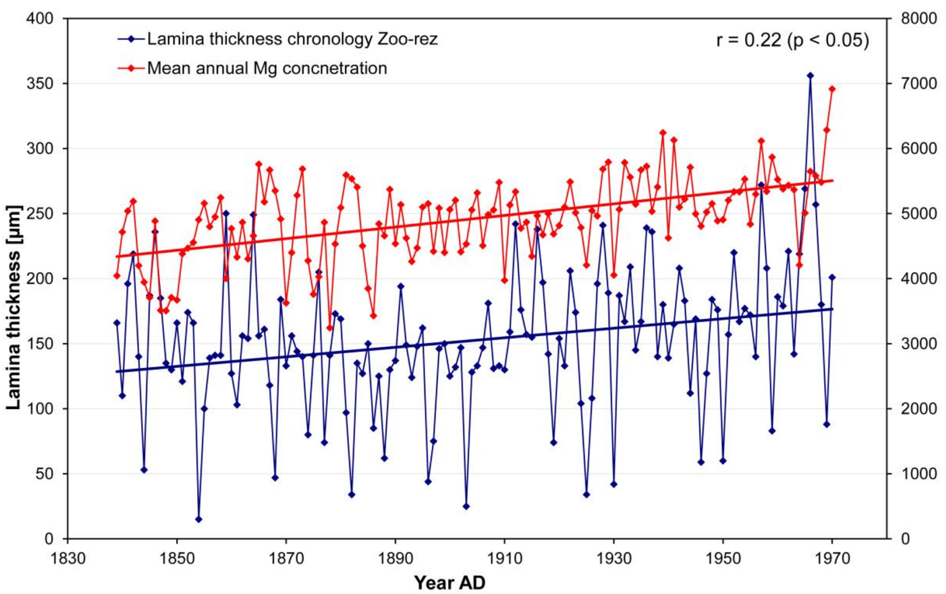

Figure 12. Comparison of lamina thickness and mean annual Mg concentration. The correlation coefficient is r = 0.22. The straight lines represent linear fits of the time series.

Clim. Past Discuss., doi:10.5194/cp-2016-18, 2016
Manuscript under review for journal Clim. Past
Published: 15 February 2016

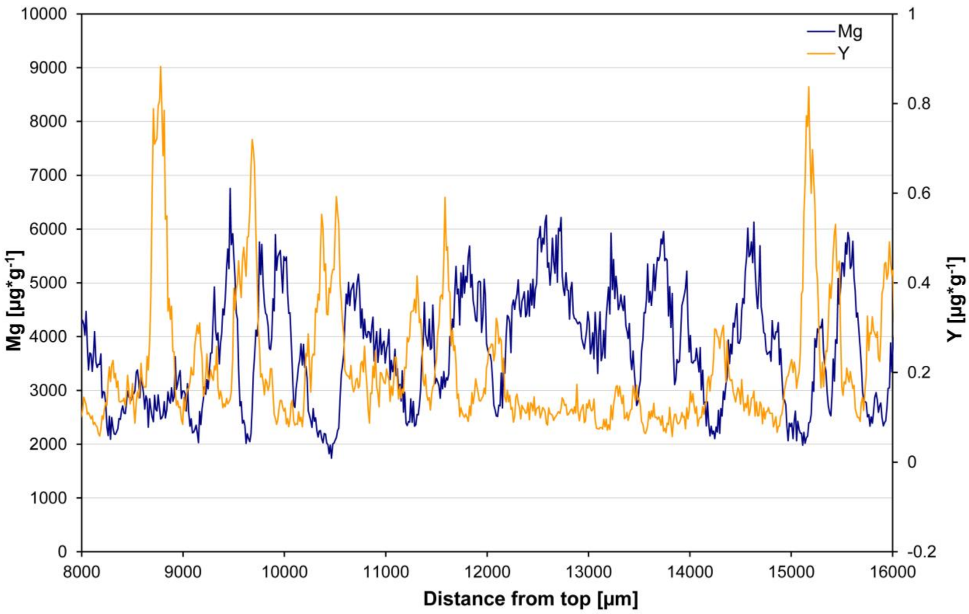

Figure 13. Evolution of Mg and Y on track Zoo-rez-2 between 8000 and16,000 µm dft.

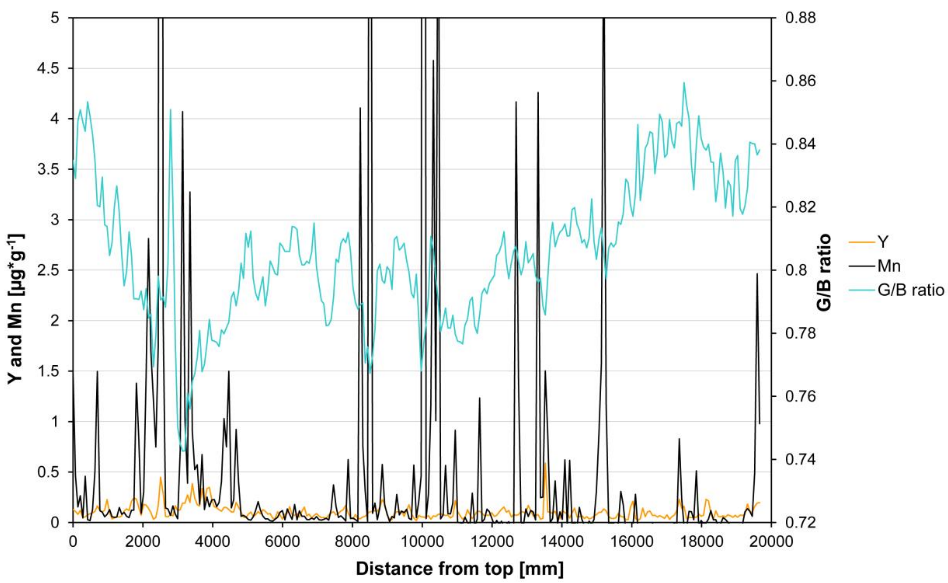

Figure 14. Comparison of the G/B ratio with the content of Y and Mn for track Zoo-rez-3.

Clim. Past Discuss., doi:10.5194/cp-2016-18, 2016
Manuscript under review for journal Clim. Past
Published: 15 February 2016

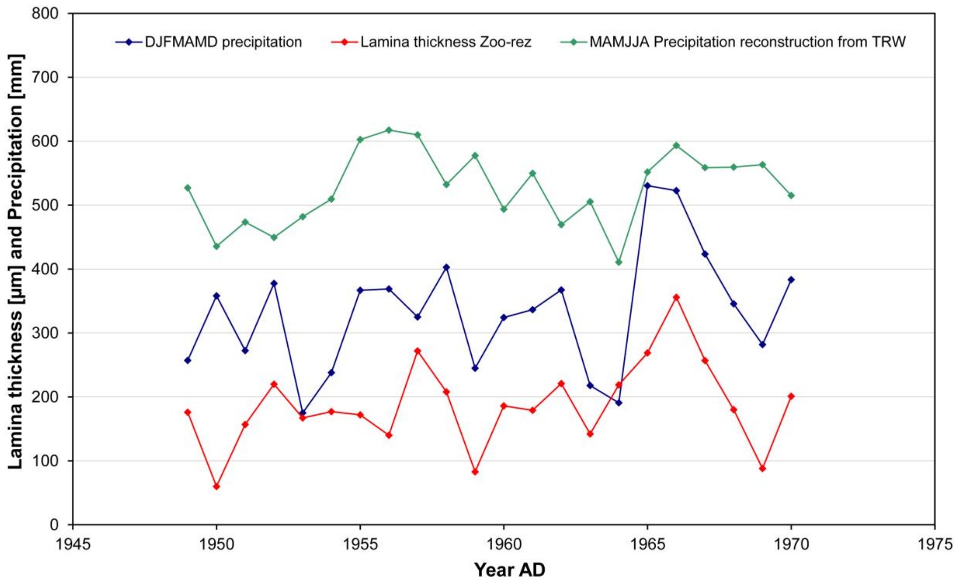

Figure 15. Comparison of the sum of the amount of precipitation during previous December, January, February, March, April, May and December (DJFMAMD) at the meteorological station Bamberg (DWD), a precipitation reconstruction for March, April, Mai, June, July, and August (MAMJJA) based on tree-ring width (Wilson et al., 2005) and the lamina thickness chronology of Zoo-rez.